

Probing the temperature of cold many-body quantum systems

Karen V. Hovhannisyanyan¹ and Luis A. Correa²

¹*Department of Physics and Astronomy, Ny Munkegade 120, 8000 Aarhus, Denmark**

²*School of Mathematical Sciences and Centre for the Mathematics and Theoretical Physics of Quantum Non-Equilibrium Systems, The University of Nottingham, University Park, Nottingham NG7 2RD, United Kingdom[†]*

(Dated: April 4, 2025)

It is well known that the uncertainty of temperature measurements on finite gapped equilibrium systems diverges exponentially fast as their temperature T drops to zero. In contrast, some exactly solvable models showcase a more benign power-law-like low- T behaviour, when only a small non-equilibrium fragment of the equilibrium system is measured. Does this mean that a part may contain more information about the global temperature than the whole? Certainly not. Here, we resolve this apparent paradox. First, we prove that local quantum thermometry at low T is *exponentially* inefficient in non-critical gapped spin and harmonic lattices. In contrast, we show through an open-system analysis that the thermal sensitivity of a harmonic thermometer (or probe) jointly equilibrated with a reservoir (or sample) by means of an Ohmic coupling scheme, displays a distinctive *power-law-like* behaviour as $T \rightarrow 0$. To reconcile these two results, we exploit the fact that local thermometry on a harmonic chain may be viewed as a temperature measurement on an oscillator in an discretized harmonic environment: A *gapped* translationally invariant chain (for which low- T thermometry is indeed exponentially inefficient) maps into a non-standard open-system model where the low-frequency modes of the sample *decouple* from the probe. On the contrary, a *gapless* instance of such chain gives rise to the canonical Ohmic probe-sample interaction, which does include sample modes of arbitrarily low frequency. In this way, we show that the power-law-like thermometric performance observed in typical dissipative models is due to the fact that these are gapless and, as such, not subjected to the exponential limitations of their gapped counterparts. The key feature of many-body systems, when it comes to the ultimate limitations of low- T thermometry, is thus whether or not their energy spectrum is gapped.

I. INTRODUCTION

Sub-micron thermometry has developed into an experimentally mature discipline, thus enabling high-resolution temperature measurements with nanometer-sized probes [1], and even individual *quantum thermometers* [2, 3]. Although measuring low temperatures with high precision is notoriously hard [4–7], the quest to produce accurate quantum thermometers fit for use in the ultra-cold regime is strongly driven by their potential applications in e.g., quantum information processing [8]. Understanding the origin of the severe fundamental limitations that hinder precise low-temperature thermometry is thus essential for future technological developments.

The temperature T of an equilibrium quantum system can be accurately calculated from a large collection of energy measurements. Indeed, knowing its spectrum and assuming that the populations in the energy basis follow a Boltzmann distribution allows to build a maximum likelihood estimator for T [9]. As it turns out, such strategy is optimal, in the sense that it achieves the smallest possible mean squared error on the estimated temperature [4]. Indeed, energy measurements allow to *saturate* the quantum Cramér-Rao inequality $(\delta T)^2 \geq 1/(M\mathcal{F}_T)$ [10] for temperature estimation on any equilibrium system. In other words, the inverse of the mean squared error of the final estimate (normalized by the length M of dataset of measurement outcomes) converges to the so-called quantum Fisher information (QFI) $\mathcal{F}_T \stackrel{M \rightarrow \infty}{\equiv} (\delta T)^{-2}/M$, which is, in our case, a quantifier of “thermal sensitivity”.

In turn, the QFI relates to the heat capacity $C(T) := d\langle H \rangle/dT$ of the equilibrium system, as $\mathcal{F}_T = C(T)/T^2$ [4, 11]. Here, H is the system Hamiltonian, $\langle \dots \rangle$ denotes thermal averaging, and we have adopted units in which $\hbar = k_B = 1$. Very generally, the heat capacity of a finite-size quantum system at equilibrium decays exponentially fast to zero in the limit $T \rightarrow 0$ [12], i.e., $C(T) \sim \mathcal{O}(e^{-\Delta/T})$, where Δ stands for the energy gap between ground and first excited states. Hence, thermometry on a finite equilibrium quantum system becomes exponentially inefficient at low temperatures [4, 13].

As the system scales up in size, its heat capacity and hence, also its thermal sensitivity, grows *extensively* (see Appendix A). However, benefiting from size-scaling would require to make generally unfeasible global multi-particle measurements, while strongly perturbing the system. This motivates the development of minimally invasive “local” thermometric strategies, aimed at inferring the global temperature from measurements on an accessible small fraction of the system [6, 14]. Note that thermometrically useful non-demolition global measurements can nevertheless be implemented in some situations [5, 15–17].

The marginal of the accessible part may deviate significantly from thermal equilibrium when it interacts strongly with the rest of the system. This is due to the large correlations built up between the two, especially at low temperatures. As a result, the internal interaction strength may be used to achieve some quantitative improvement over the local equilibrium situation. Nonetheless, whenever the global system is gapped, translationally invariant, short-range interacting, and non-critical, the exponential *scaling* at low temperatures is inescapable, as we will prove in Sec. II A.

One may adopt an open-system perspective to tackle the

* karen@phys.au.dk

† luis.correa@nottingham.ac.uk

problem of local thermometry [13], since the dissipative dynamics of an individual quantum *probe* coupled to an initially thermal and large *sample*, converges to a global equilibrium state [18]. In this sense, “probe” and “sample” match the “accessible” and “inaccessible” parts of the many-body system in the setting outlined above. In particular, linear open quantum systems are especially interesting, as the reduced steady state of the probe can be found *exactly* [18, 19].

Following this approach, we were able to establish in Ref. [13] that $\mathcal{F}_T \sim T^2$ in the limit $T \rightarrow 0$, for the simplest model of Brownian motion, i.e., a single harmonic thermometer coupled to an initially thermal bosonic reservoir [20–22]. Our results followed from the exact analytical steady-state solution, and indicated that such power-law-like scaling holds for various instances of Ohmic and super-Ohmic spectral densities. In Sec. II B, we will rigorously prove that a power-law-like scaling is indeed a signature of the ubiquitous Ohmic dissipation scheme: On confined probes we find a quadratic asymptotic scaling $\mathcal{F}_T \sim T^2$, while the diverging behaviour $\mathcal{F}_T \sim 1/T^2$ is characteristic of (quasi-)free thermometers.

This exact result seems to be in stark contradiction with the discussion above: How can a (tiny) subsystem display a power-law-like decaying thermal sensitivity if global thermometry on the whole should be exponentially inefficient? The answer is that this model is *gapless* and hence, fundamentally different from gapped systems. Namely, gapless systems are necessarily infinite, i.e., large enough to justify taking the thermodynamic limit. In addition, they do not have a parameter akin to the spectral gap Δ , that would set an energy scale.

In order to gain physical insight, we turn to quantum harmonic systems. Specifically, we will consider 1D translationally invariant harmonic chains (TIHCs) with linear (but not necessarily short-range) interactions, prepared in thermal equilibrium. It is easy to verify that local thermometry, on a single node of a gapped instance of the chain, is exponentially inefficient, while power-law-like behaviour shows up when a vanishing gap is enforced (see Sec. III). We then try to look at such TIHCs from an open-system perspective: We diagonalize the inaccessible part so as to bring the problem into an equivalent open-system-like “star” configuration, where the probe is surrounded by non-interacting peripheral sample modes. Gapped chains map into open systems with unusual spectral densities, where the low frequency sample modes appear decoupled from the probe. On the other hand, gapless chains give rise to standard Ohmic spectral densities, as we shall argue in Sec. IV. Hence, a gapless TIHC maps into the paradigmatic Caldeira-Leggett model (CLM) [20] in the thermodynamic limit (cf. IV A). Conversely, in IV B we illustrate that local thermometry on an Ohmic Brownian motion model is equivalent to local thermometry on a gapless TIHC.

Quite intuitively, this open-system viewpoint indicates that the ability of the probe to detect near-ground-state temperature fluctuations crucially depends on whether or not it is effectively coupled to the lowermost normal modes of the sample, which, in turn, are the only ones that may be thermally populated at very low T [6, 13]. Our findings (summarized and elaborated in Sec. V) imply that engineering the probe-sample thermal coupling to guarantee a good thermal con-

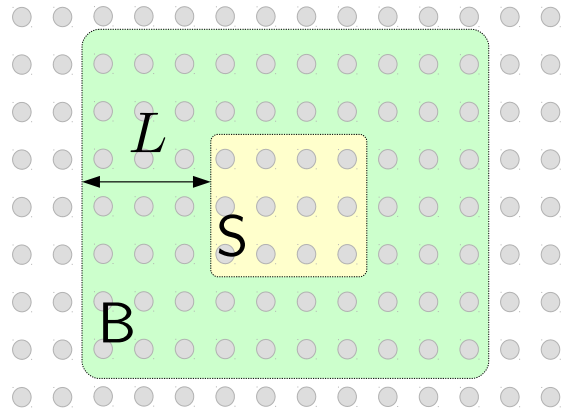


FIG. 1. (color online) Schematic diagram of a 2D translationally invariant lattice. The system S and the boundary B (of length L) appear depicted in yellow and green, respectively. Although not shown, the nodes (gray dots) of the lattice are connected by short-ranged interactions. It is also assumed that the many-body system is away from criticality.

tact with the low-frequency modes of the sample is the key to precise low-temperature quantum thermometry. In this sense, reservoir engineering and dynamical control [23] could come to play a major role in practical technological applications.

II. EXPONENTIAL VS. POWER-LAW-LIKE DECAY OF THERMOMETRIC PERFORMANCE AT LOW T

A. Exponential inefficiency of local quantum thermometry in gapped lattice systems

Here, we shall consider the problem of local thermometry on an equilibrium lattice of identical harmonic oscillators or spins at temperature T . To be precise, we will look at arbitrarily large translationally-invariant gapped lattices, away from criticality, and featuring short-range interactions. Our task will be to infer the global temperature T from local observations on the (non-equilibrium) marginal of a finite-size subsystem S . Two conflicting factors are at play here: On the minus side, the temperatures are low and S is of finite size, which makes us expect exponentially inefficient thermometry. However, S is *strongly correlated* with the rest of the lattice, which due to its size, has an overall large heat capacity. We will show that the first factor nevertheless prevails and the thermal sensitivity decays exponentially, namely as

$$\mathcal{F}_T \leq \mathcal{O}(1)e^{-\beta\Delta} \quad (\text{for } \beta\Delta \gg 1), \quad (1)$$

where the QFI \mathcal{F}_T is adopted as the figure of merit. This can be formally defined as

$$\mathcal{F}_T = -2 \lim_{\delta \rightarrow 0} \frac{\partial^2 \mathbb{F}(\rho_T, \rho_{T+\delta})}{\partial \delta^2}, \quad (2)$$

where ρ_θ denotes the marginal of S when the global lattice is at temperature θ and $\mathbb{F}(\rho, \sigma) := (\text{tr} \sqrt{\sqrt{\rho} \sigma \sqrt{\rho}})^2$ is the Uhlmann fidelity between states ρ and σ [24]. Note how, already from its definition, it is intuitively clear that \mathcal{F}_T gauges the *responsiveness* of the probe to small fluctuations in the sample temperature. For convenience, we shall cast \mathcal{F}_T in the equivalent form (cf. Appendix B)

$$\mathcal{F}_T = 4 \lim_{\delta \rightarrow 0} \frac{1 - \mathbb{F}(\rho_T, \rho_{T+\delta})}{\delta^2}, \quad (3)$$

so that $\mathbb{F}(\rho_T, \rho_{T+\delta}) = 1 - \frac{1}{4} \mathcal{F}_T \delta^2 + \mathcal{O}(\delta^3)$ and hence, the Bures distance $d_B^2(\rho_T, \rho_{T+\delta}) := 2 \left(1 - \sqrt{\mathbb{F}(\rho_T, \rho_{T+\delta})} \right)$ becomes

$$d_B^2(\rho_T, \rho_{T+\delta}) = \frac{1}{4} \mathcal{F}_T \delta^2 + \mathcal{O}(\delta^3). \quad (4)$$

In what follows, we will use general arguments on locality of temperature [25–27] to bound the left-hand side of Eq. (4) from above and thus, extract the low- T scaling of \mathcal{F}_T .

Let us denote the number of sites, i.e., the “size” of the system, by L_S and introduce a *boundary region* around it, of size L (see Fig. 1). Also let $\tau_T(L_S + L)$ be a thermal state at temperature T defined from the local Hamiltonian of “system + boundary” and $\rho_T(L) := \text{tr}_B \tau(L_S + L)$, the reduction of $\tau_T(L_S + L)$ within S . By definition, one thus has $\rho_T(L) \stackrel{L \rightarrow \infty}{=} \rho_T$. From the triangle inequality, it follows that

$$d_B(\rho_T, \rho_{T+\delta}) \leq d_B(\rho_T(L), \rho_{T+\delta}(L)) + d_B(\rho_T, \rho_T(L)) + d_B(\rho_{T+\delta}, \rho_{T+\delta}(L)). \quad (5)$$

We can now use the data-processing inequality for the Bures distance [28] to bound the first term of the right-hand side as $d_B(\rho_T(L), \rho_{T+\delta}(L)) \leq d_B(\tau_T(L_S + L), \tau_{T+\delta}(L_S + L))$. According to Eq. (4), the latter can be cast as $\frac{1}{2} \sqrt{\mathcal{F}_T(L_S + L)} \delta + \mathcal{O}(\delta^2)$ and, since $\tau_T(L_S + L)$ is a thermal state, we may additionally exploit the relation $\mathcal{F}_T(L_S + L) = C_{S+B}(T)/T^2$, where $C_{S+B}(T)$ is the heat capacity of the “system + boundary” composite. Hence, we finally arrive at

$$d_B(\rho_T, \rho_{T+\delta}) \leq \frac{\sqrt{C_{S+B}(T)}}{2T} \delta + d_B(\rho_T, \rho_T(L)) + d_B(\rho_{T+\delta}, \rho_{T+\delta}(L)) + \mathcal{O}(\delta^2). \quad (6)$$

Focusing now on the locally finite case (i.e., each node has a finite-dimensional Hilbert state space) and, given that we work with short-range-interacting systems away from criticality, we may use the results of Refs. [25–27] about approximating $\rho_T = \rho_T(\infty)$ by $\rho_T(L)$ for finite but large L . In Ref. [27] it was shown that, for such systems in 1D

$$\mathbb{F}(\rho_T(L), \rho_T) = 1 - \mathcal{O}(1) e^{-L/\xi(T)}, \quad (7)$$

where $\xi(T)$ is a monotonic function of the correlation length of the infinite chain, and, since the system is away from criticality, $\xi(T)$ is also a regular function of T , even when $T \rightarrow 0$. In terms of Bures distance, we can thus write

$$d_B(\rho_T(L), \rho_T) = \mathcal{O}(1) e^{-\frac{L}{2\xi(T)}}. \quad (8)$$

Let us define $\xi := \max\{\xi(T), \xi(T + \delta)\}$, so that Eq. (6) can be cast as

$$d_B(\rho_T, \rho_{T+\delta}) \leq \frac{\sqrt{C_{S+B}(T)}}{2T} \delta + \mathcal{O}(1) e^{-\frac{L}{2\xi}} + \mathcal{O}(\delta^2). \quad (9)$$

In Appendix A, we argue that the heat capacity of gapped locally finite translationally invariant lattices with nearest-neighbour interactions, and that of harmonic, translationally invariant, and not necessarily short-range interacting many-body systems, scales as

$$C_{S+B}(T) = \mathcal{O}\left(N e^{-\beta\Delta}\right), \quad (10)$$

which leads us to

$$d_B(\rho_T, \rho_{T+\delta}) \leq \mathcal{O}(1) \left[\sqrt{L_S + L} e^{-\frac{\beta\Delta}{2}} \delta + e^{-\frac{L}{2\xi}} + \delta^2 \right]. \quad (11)$$

Furthermore, in Appendix A 2 the scaling in Eq. (10) is illustrated in the quantum Ising model.

Since we are interested in the low-temperature regime, we shall take the limit $\beta\Delta \rightarrow \infty$. Therefore, we must ensure that δ is much smaller than T (so that our Taylor expansions above make sense). Let us thus choose $\delta = \Delta e^{-\beta\Delta}$, which, as needed, satisfies $\delta/T = (\beta\Delta) e^{-\beta\Delta} \ll 1$. Furthermore, let $L = 4\xi\beta\Delta$ [so that $L \gg 1$, as it was necessary for Eq. (8)]. Substituting these into (11), we arrive at

$$d_B(\rho_T, \rho_{T+\delta}) \leq \mathcal{O}(1) \left(e^{-\frac{3}{2}\beta\Delta} + \delta^2 \right) = \mathcal{O}(1) e^{-\frac{3}{2}\beta\Delta}, \quad (12)$$

which, due to Eq. (4), leaves us with Eq. (1). We have thus shown that, very generally, local thermometry is exponentially inefficient at low temperatures in arbitrarily strongly but short-range interacting lattices.

Although our proof is rigorous only in 1D, we expect Eq. (1) to be widely applicable also in higher dimensions. Indeed, except for Eq. (7), all the steps in the proof hold in any spatial dimension. When it comes to Eq. (7), the results in Ref. [26] support the general intuition that it should generically apply to lattices with locally finite-dimensional Hilbert spaces, that are away from criticality, irrespective of spatial dimension. Furthermore, the results in [29] about approximating $\rho_T(\infty)$ with $\rho_T(L)$, those of Ref. [30] about the relation between the spectral gap and exponential decay of correlations in generic harmonic lattices, and our Appendix A strongly suggest that Eq. (1) should also be applicable in generic harmonic lattice systems in any dimension.

B. Power-law-like sensitivity of a Brownian thermometer coupled to a sample through an Ohmic interaction

In this section, we will consider the low-temperature scaling of the sensitivity of a Brownian quantum particle. To that end, we shall adopt the quintessential Caldeira-Leggett model [19, 20], consisting of a quantum harmonic thermometer of bare frequency ω_0 , linearly coupled to a bosonic reservoir (playing the role of the “sample”) through an Ohmic interaction scheme. The sample will be initially prepared in thermal equilibrium at some unknown temperature T (to be measured). The probe, on the other hand, may be initialized in

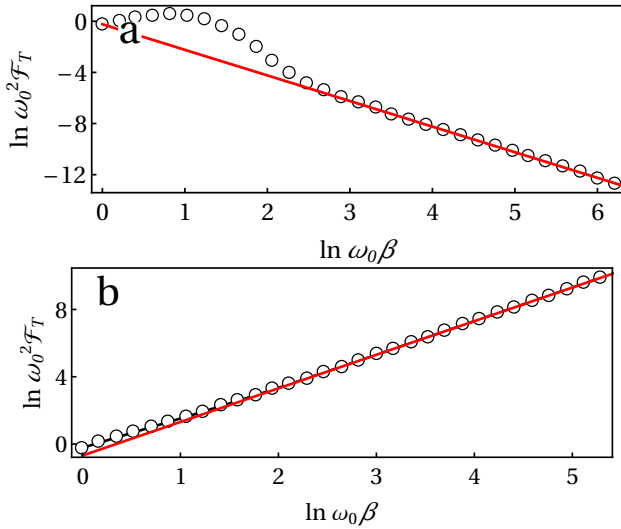


FIG. 2. (color online)(a) Log-log plot of the QFI as a function of the inverse temperature $\beta = 1/T$ (open circles) for a trapped probe ($\omega_0 \neq 0$). The low-temperature asymptotic behaviour $\mathcal{F}_T \sim T^2$ appears superimposed in red. (b) Same as in (a) but for a free probe ($\omega_0 \rightarrow 0$). In this case, the low- T scaling is $\mathcal{F}_T \sim 1/T^2$ (red). In (a) $\omega_0 = 1$, while in (b), $\omega_0 = 10^{-3}$. In the two panels, we chose $\gamma = 0.1$ and $\omega_c = 100$. Note that, in both cases, the power-law-like scalings are maintained well beyond the bounds in Eqs. (19).

an arbitrary state, so long as it starts uncorrelated from the sample. The dissipative dynamics following from the thermal contact between probe and sample will bring the composite to a global equilibrium state at temperature T [18].

The Caldeira-Leggett Hamiltonian H_{CL} , reads

$$H_{\text{CL}} = \frac{p_0^2}{2} + \frac{1}{2}(\omega_0^2 + \omega_R^2) \frac{q_0^2}{2} + q_0 \sum_{\mu} g_{\mu} q_{\mu} + \sum_{\mu} \left(\frac{p_{\mu}^2}{2} + \frac{q_{\mu}^2 \omega_{\mu}^2}{2} \right), \quad (13)$$

where (q_0, p_0) are the position and momentum quadratures of the probe, (q_{μ}, p_{μ}) are those of mode ω_{μ} in the sample, and the g_{μ} stand for the probe-sample coupling strengths. The term $\omega_R^2 := \sum_{\mu} g_{\mu}^2 / \omega_{\mu}^2$ needs to be added “by hand” in order to ensure that H_{CL} is positive-definite [19]. Note that, since H_{CL} is quadratic, the steady state of the probe will be Gaussian and thus, completely described by the elements of the covariance matrix $[\sigma_T]_{ij} := \frac{1}{2} \langle \{R_i, R_j\}_+ \rangle$, where $\vec{R}^T = (q_0, p_0)$ and $\{\cdot, \cdot\}_+$ denotes anticommutator (note that the first moments of a Brownian particle vanish, i.e., $\langle q_0 \rangle = \langle p_0 \rangle = 0$).

The central quantity describing the probe-sample interaction is the *spectral density*

$$J(\omega) = \pi \sum_{\mu} \frac{g_{\mu}^2}{\omega_{\mu}} \delta(\omega - \omega_{\mu}). \quad (14)$$

Some popular profiles for $J(\omega)$ are the Ohmic spectrum with Lorentz-Drude cutoff, i.e., $J(\omega) = 2\gamma\omega\omega_c^2/(\omega^2 + \omega_c^2)$, which makes it particularly easy to obtain explicit analytical formulas for the steady state of the probe [13, 31]; or the case of

variable “Ohmicity” s and exponential cutoff, i.e., $J_s(\omega) = \frac{\gamma\pi}{2} (\omega^s / \omega_c^{s-1}) e^{-\omega/\omega_c}$ [32]. Whenever $s > 1$ we talk about super-Ohmic spectra, whereas the choice $s < 1$ corresponds to the sub-Ohmic case. The most general Ohmic spectral density ($s = 1$) should be of the form

$$J(\omega) = \gamma\omega f(\omega/\omega_c), \quad (15)$$

where γ is the so-called dissipation rate and $f(x) > 0$ is a dimensionless function that starts to decay rapidly to 0 as soon as $x > 1$, and that is smooth around $x = 0$, with $f(0) = 1$. The cutoff ω_c places a cap on the frequency of the modes in the (infinite) sample that are *effectively* coupled to the probe.

Remarkably, general closed-form analytical expressions can be derived for the steady-state covariance matrix [19]:

$$[\sigma_T]_{11} = \frac{1}{2\pi} \int_0^{\infty} d\omega \frac{J(\omega)}{|\alpha(\omega)|^2} \coth \frac{\omega}{2T} \quad \text{and} \quad (16a)$$

$$[\sigma_T]_{22} = \frac{1}{2\pi} \int_0^{\infty} d\omega \frac{\omega^2 J(\omega)}{|\alpha(\omega)|^2} \coth \frac{\omega}{2T}, \quad (16b)$$

while $[\sigma_T]_{12} = [\sigma_T]_{21} = 0$. The *susceptibility* $\alpha(\omega)$ is

$$\alpha(\omega) := \omega_0^2 + \omega_R^2 - \omega^2 - J(\omega) - i\chi(\omega), \quad (17)$$

where $\chi(\omega) = \frac{1}{\pi} \text{P} \int_{-\infty}^{\infty} d\omega' \frac{\tilde{J}(\omega')}{\omega' - \omega}$ is the Hilbert transform [33] of the spectral density, extended as an odd function for negative frequencies, i.e., $\tilde{J}(\omega) := J(\omega)\Theta(\omega) - J(-\omega)\Theta(-\omega)$. Here, $\Theta(\omega)$ is the Heaviside step function, and P denotes the Cauchy principal value of the integral.

Using the definition of \mathcal{F}_T in Eq. (2) in combination with the formula for the Uhlmann fidelity between two single-mode Gaussian states in terms of their 2×2 covariance matrices σ and σ' [34]

$$\mathbb{F}(\sigma, \sigma') = \frac{2}{\sqrt{\Lambda + \Delta} - \sqrt{\Lambda}}, \quad \text{with} \quad (18)$$

$$\Lambda := (4 \det \sigma - 1)(4 \det \sigma' - 1)$$

$$\Delta := 4 \det(\sigma + \sigma'),$$

and Eqs. (16) and (17), we can rigorously prove the following asymptotic behaviours for the QFI under the generic Ohmic spectral density of Eq. (15):

- (i) For $\omega_0 \neq 0$ and in the limit $T \ll \omega_0^4 \omega_c^{-3}$

$$\mathcal{F}(T) \sim T^2 \quad (19a)$$

- (ii) and for a free particle ($\omega_0 = 0$) at $T \ll \omega_c$

$$\mathcal{F}(T) \sim 1/T^2. \quad (19b)$$

While all details are deferred to Appendix C, here we illustrate Eqs. (19) in Fig. 2. Note that, in contrast with the results from Sec. II A, the low- T scaling of \mathcal{F}_T is not exponential, but power-law-like. As already advanced in Sec. I, the scaling (19a) had been established by us in Ref. [13] for exponential and Lorentzian cutoff functions. Interestingly, the same T^2 scaling was recently reported also in a gapless fermionic tight

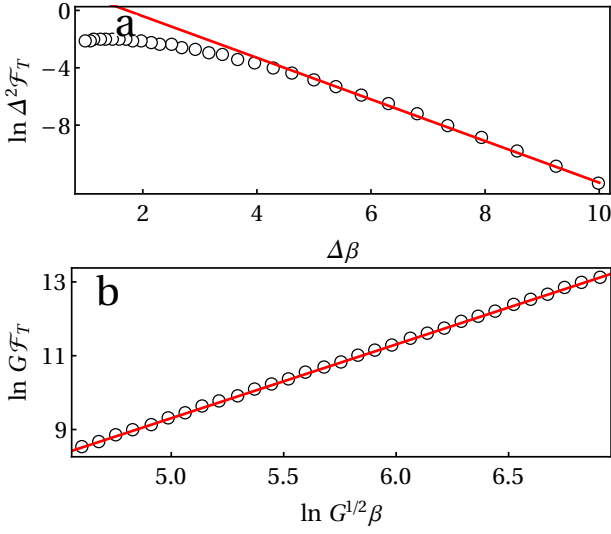


FIG. 3. (color online) (a) Log plot of the QFI as a function of the inverse temperature β (open circles) for a gapped translationally-invariant harmonic chain with gap $\Delta = 0.01$. The exponential asymptotic scaling $\mathcal{F}_T \sim e^{-\Delta/T}$ has been superimposed in red. In this case $N = 100$ and the interactions have been chosen as $G_n = G/n^t$, with $G = 1$ and $t = 2.5$. For these parameters, the corresponding bare oscillator frequency is $\Omega^2 \simeq 1.73425$. (b) Log-log plot of the QFI versus the inverse temperature β . All parameters are the same as in (a) except for $\Omega^2 \simeq 1.73435$, chosen so that the TIHC is gapless. The power-law-like divergence $\mathcal{F}_T \sim 1/T^2$ (or constant relative error $\sqrt{M}\delta T/T$) of Eq. (19b) has been plotted in red.

binding chain in 1D [35]. Note as well that the best-case relative error $\frac{\delta T}{T} \sim \frac{1}{T\sqrt{M\mathcal{F}_T}}$ diverges as $T \rightarrow 0$ in the case of a confined Brownian thermometer, i.e., $\omega_0 \neq 0$ [13]. However, in Fig. 2(b) we see that it may be kept *constant* over a wide range of arbitrarily low temperatures, by choosing $\omega_0 \rightarrow 0$. The same behaviour has been recently observed on a dynamically-controlled probe in Ref. [23].

III. LOCAL THERMOMETRY ON GAPPED AND GAPLESS HARMONIC CHAINS

The aim of this section is to illustrate that having either a finite or a vanishing spectral gap in a system, is the key factor which determines whether the performance of local thermometry on will scale exponentially (as in Sec. II A) or as a power law (as in the family of open-system models of Sec. II B), when $T \rightarrow 0$. Our workhorse will be a 1D chain of $2N + 1$ identical harmonic oscillators of frequency Ω , i.e., a TIHC, prepared at temperature T (the reason for choosing $2N + 1$ nodes will become clear in Sec. IV). Let its Hamiltonian be

$$H_C = \sum_{i=1}^{2N+1} \left(\frac{P_i^2}{2} + \frac{\Omega^2}{2} Q_i^2 \right) + \frac{1}{2} \sum_{i \neq k} G_{ik} Q_i Q_k = \frac{1}{2} \vec{P}^T \vec{P} + \frac{1}{2} \vec{Q}^T V_C \vec{Q}, \quad (20)$$

where (Q_i, P_i) are the quadratures of each oscillator (collected in the $2N + 1$ -dimensional vectors \vec{Q} and \vec{P}), and G_{ik} are their mutual couplings. We will assume that these depend only on the “distance” between nodes, i.e., $G_{ij} = G_{|i-j|}$ and will impose periodic boundary conditions $G_n = G_{2N+1-n}$ for $1 \leq n \leq 2N$, which results in a *circulant* interaction matrix V_C [36], the first row of which is $(\Omega^2, G_1, \dots, G_N, G_N, G_{N-1}, \dots, G_1)$. The eigenvalues of the interaction matrix (i.e., the squared normal mode frequencies of the system) are

$$\Omega_a^2 = \Omega^2 + 2 \sum_{k=1}^N G_k \cos \left(\frac{2\pi ka}{2N+1} \right), \quad \text{for } a = 0, \dots, 2N, \quad (21)$$

where we notice that the frequencies $\Omega_{N+1}, \dots, \Omega_{2N}$ coincide with $\Omega_N, \dots, \Omega_1$, respectively.

In Sec. IV below, we will comment further on the choice of the inter-node couplings. For now, we will just assume that their strength decreases with the distance, i.e., $G_i > G_j > 0$ for $i < j$. In this case, the fundamental mode of the system has squared frequency Δ^2 such that

$$\Delta^2 = \Omega_N^2 = \Omega^2 + 2 \sum_{k=1}^N G_k \cos \left[\frac{2\pi kN}{2N+1} \right]. \quad (22)$$

Therefore, for the system’s spectrum to be bounded from below, one must have

$$\Omega^2 \geq -2 \sum_{k=1}^N G_k \cos \left[\frac{2\pi kN}{2N+1} \right]. \quad (23)$$

The strict inequality gives rise to a *gapped* TIHC, whereas its saturation yields a *gapless* system.

We will now evaluate the QFI of a single node of the chain (say node #1, as they are all equivalent) both in the gapped and the gapless case. To that end, we need to compute the elements of its reduced covariance matrix, i.e. $[\sigma_T]_{11} = \langle Q_1^2 \rangle$ and $[\sigma_T]_{22} = \langle P_1^2 \rangle$ ($[\sigma_T]_{12} = [\sigma_T]_{21} = \frac{1}{2} \langle \{Q_1, P_1\}_+ \rangle = 0$). Letting $\vec{q}^C = O_C \vec{Q}$ be the normal mode quadratures, these write as

$$[\sigma_T]_{11} = \sum_{j=1}^{2N+1} [O_C^T]_{1j}^2 \frac{1}{2\Omega_{j-1}} \coth \frac{\Omega_{j-1}}{2T} \quad (24a)$$

$$[\sigma_T]_{22} = \sum_{j=1}^{2N+1} [O_C^T]_{1j}^2 \frac{\Omega_{j-1}}{2} \coth \frac{\Omega_{j-1}}{2T}. \quad (24b)$$

From Eqs. (2), (18), and (24), one can calculate the corresponding local QFI. In Fig. 3, we work out a 100-node example: As it can be seen, when the chain is gapped, the low- T sensitivity decays exponentially, as expected from Sec. II A [see Fig. 3(a)]. However, when the system is tuned to be gapless, it exhibits a power-law-like divergence of the type $\mathcal{F}_T \sim 1/T^2$ [see Fig. 3(b)]. In view of the results of Sec. II B, this observation could be the “smoking gun” of a deeper connection between local thermometry on many-body lattices and open system-models. We will now follow this lead by characterizing the open-system-like analogue of a single node within gapped and gapless TIHCs.

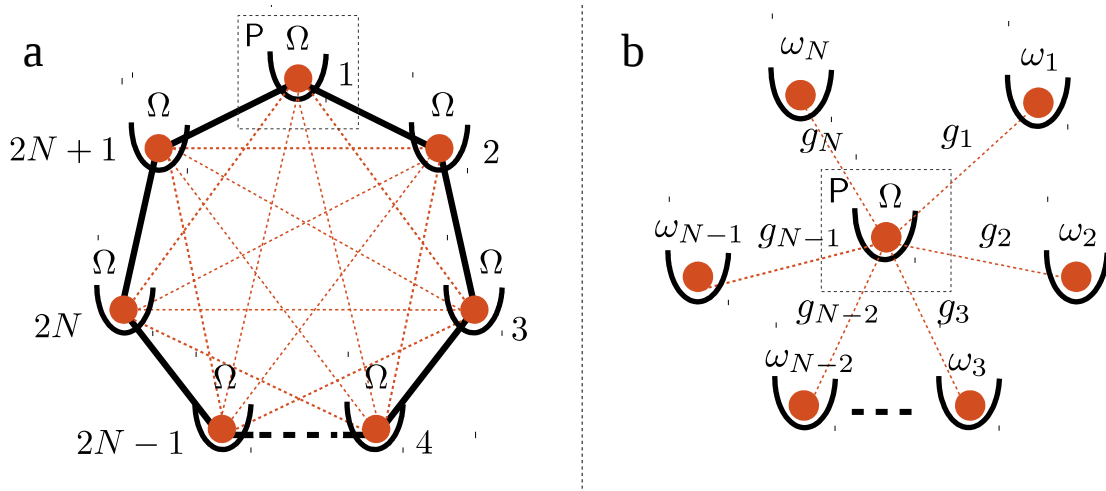


FIG. 4. (color online) (a) Sketch of a translationally invariant Harmonic chain with periodic boundary conditions and $2N+1$ nodes of frequency Ω . Node #1 appears highlighted as the probe P . This corresponds to Eq. (20). (b) Equivalent “star” system, described by Eq. (26), where node #1 couples to N of the two-fold degenerate normal modes of the inaccessible part of the chain, with frequencies ω_i .

IV. MAPPING A TRANSLATIONALLY INVARIANT HARMONIC CHAIN INTO A “STAR” MODEL AND BACK

A. From a harmonic chain to a star model

We shall start by splitting the Hamiltonian H_C of the TIHC in Eq. (20) into its accessible (i.e., node #1) and inaccessible parts (i.e., all other nodes), and the interactions between the two. That is,

$$H_C = \frac{1}{2}(P_1^2 + \Omega^2 Q_1^2) + Q_1 \sum_{i>1} G_{1i} Q_i + \frac{1}{2} \sum_{i>1} (P_i^2 + \Omega^2 Q_i^2) + \frac{1}{2} \sum_{\substack{i \neq k \\ i, k > 1}} Q_i [V_{1|C}]_{ik} Q_k, \quad (25)$$

where the $2N \times 2N$ matrix $V_{1|C}$ results from removing the first row and column from V_C . Note that $V_{1|C}$ is thus not circulant ($G_{2N-1} = G_2 \neq G_1$) but a symmetric Toeplitz matrix [36].

Let us denote $\vec{Q}_{1|C}^T := (Q_2, \dots, Q_{2N+1})$. Provided that the real orthogonal matrix $O_{1|C}$ diagonalizes $V_{1|C}$ (i.e., $O_{1|C} V_{1|C} O_{1|C}^T = \text{diag}\{\omega_1^2, \dots, \omega_{2N}^2\}$), we define the *sample* degrees of freedom from the normal-mode coordinates of the inaccessible nodes $\vec{q}^{1|C} := O_{1|C} \vec{Q}_{1|C}$. Eq. (25) thus rewrites as

$$H_C = \frac{1}{2}(P_1^2 + \Omega^2 Q_1^2) + Q_1 \sum_{i>1} g_i q_i^{1|C} + \frac{1}{2} \sum_{i>1} [(p_i^{1|C})^2 + \omega_i^2 (q_i^{1|C})^2]. \quad (26)$$

The transition between the chain-like model of Eq. (25) and the star-like configuration of Eq. (26) is depicted in Fig. 4.

Note that the transformed coupling constants are given by $g_i = [O_{1|C}]_{ij} G_{1j}$. As it turns out, the probe interacts only with *half* of the sample modes due to the existing symmetries. Therefore, we shall keep only the N relevant ones and define

the effective spectral density as $J(\omega) = \pi \sum_{i=1}^N \frac{g_i^2}{\omega_i} \delta(\omega - \omega_i)$, which will be the central object of interest in what follows.

As illustrated in Fig. 5, whenever G_n decays as n^{-1} or faster, the spectral density is approximately linear around its minimal frequency, which is non-zero. Hence, gapped TIHCs are not capable of reproducing the canonical Ohmic form of Eq. (15) in their residual spectra. In any case, they are endowed with a high-frequency cutoff.

In the limit of large N , the chain is gapless for $\Omega^2 = 2 \sum_{n=1}^{\infty} (-1)^{n-1} G_n$ as follows from the saturation of Eq. (23) (see also Appendix D), and the effective spectral density becomes truly Ohmic (see Fig. 5). We note that a closing gap also implies $\Omega^2 = \omega_R^2$, where the Caldeira-Leggett renormalization frequency had been introduced in Sec. II B.

These facts leave us with the following picture: Whenever the internal couplings in a gapless TIHC decay at least as fast as the inverse of the distance between the nodes, the interac-

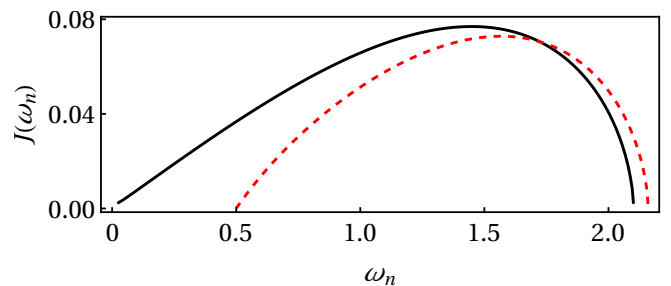


FIG. 5. (color online) Effective spectral densities after partitioning an $N = 100$ TIHC as “node #1” versus the rest. The interactions G_n are the same as in Fig. 3. We plot both the gapless (solid black) and the gapped case (dashed red), with gap $\Delta = 0.5$ (i.e., $\Omega^2 \simeq 1.98425$). Note that in both situations $J(\omega)$ shows an approximately linear growth for low ω_n and features a cutoff. In the gapped case, however, the lowest sample mode coupled to the probe has a finite frequency and hence, the resulting spectral density is *not* Ohmic.

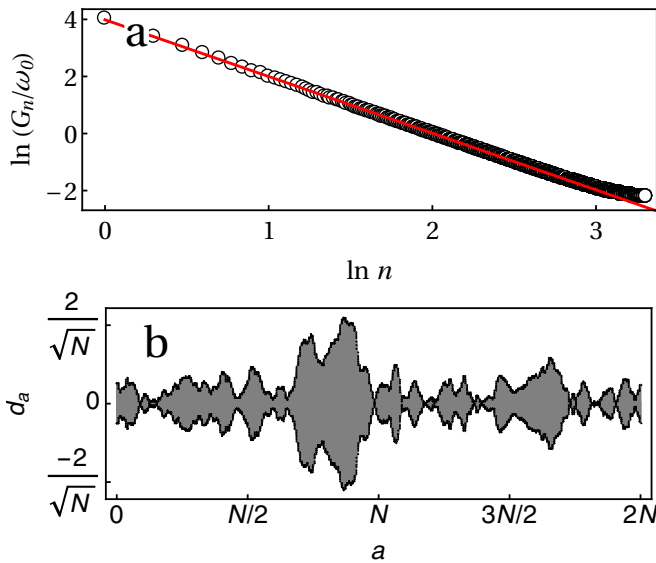


FIG. 6. (color online) **(a)** Log-log plot of the coupling constants G_n (open circles) corresponding to a discretized Caldeira-Leggett model with Ohmic spectral density and Lorentz-Drude cutoff, as a function of the inter-node distance n . In particular, the spectral density is characterized by $\gamma = 0.1$ and $\omega_c = 2$. A total of $N = 2000$ frequencies were uniformly picked within the interval $\omega_n \in (0, \omega_{\max})$, with $\omega_{\max} = 100$. The frequency of the probe was chosen as $\omega_0 = 0.2$. A linear fit $G_n \sim n^{-c}$ with $c \simeq 1.98803$ (red) has been added for comparison (see text for further details). **(b)** Coefficients of the expansion $q_0 = \sum_a d_a Q_a$ of the position of the probe in the CLM as a linear combination of the positions of the oscillators in the corresponding TIHC. All parameters are the same as in (a).

tion of every node with the rest of the chain is described by an Ohmic CLM, in which the probe has vanishing frequency $\omega_0 \rightarrow 0$. This means that Eq. (19b) can be directly applied when the temperature of cold TIHC is to be estimated by measuring a single node which is, in turn, consistent with our observations in Fig. 3(b). Even if we illustrate this by resorting to a specific example, we have numerically explored a large range of TIHCs: In addition to the standard choices of algebraic (i.e., $G_n \propto n^{-t}$ for $t > 0$, as in Fig. 3) and exponential ($G_n \propto e^{-cn}$ for $c > 0$) interactions, we have run tests using ordered lists of random numbers as coupling constants. In all cases, the results were qualitatively the same, which makes us confident that they hold in general.

B. From a star model to a harmonic chain

In this section we will consider the reverse problem—finding a TIHC that corresponds to a given (discretized) CLM. At the most basic level, one wants to ensure that there exists a TIHC with the same set of normal modes as the linear open-system at hand. However, the probe in the CLM will not correspond, in general, to one of the nodes of its associated TIHC. Rather, it will be *delocalized* over some (or all) of its nodes. This is due to the fact that the canonical transformations diagonalizing both systems are generally different. It is

thus interesting to determine how does local thermometry on a CLM look from the perspective of its TIHC analogue.

Let us return for a moment to Sec. III and recall that all but one (namely, the largest, Ω_0) of the normal modes of a $2N + 1$ -node TIHC are doubly degenerate. We can define the $N + 1$ -dimensional vectors $\vec{\Omega}^T := (\Omega_0^2, \Omega_1^2, \dots, \Omega_N^2)$ and $\vec{G}^T := (\Omega^2, 2G_1, \dots, 2G_N)$, containing the non-repeated normal-mode squared frequencies, and the squared “physical” frequency and interaction strengths, respectively. Hence, we may rewrite Eq. (21) in compact form as $\vec{\Omega} = A\vec{G}$, where $[A]_{jk} = \cos(\frac{2\pi jk}{2N+1})$, for $j, k = 0, \dots, N$.

Proceeding from the other end, we may calculate the normal mode frequencies of the $N + 1$ -particle CLM under consideration and arrange them in decreasing order in the vector $\vec{\omega}^T := (\omega_0^2, \dots, \omega_N^2)$. All we have to do is to invert the above relation, i.e., $\vec{G} = A^{-1}\vec{\omega}$, so that the resulting \vec{G} fully characterizes the TIHC matching our CLM.

In order to put the above into practice, we need to discretize a CLM. We start by setting a cap on the sample frequencies $\omega_{\max} > \omega_c$ and distributing our frequencies uniformly over the allowed range. In order to obtain the coupling g_n for any given ω_n , one may use the relation

$$g_n^2 = \frac{\omega_n}{\pi} \int_{\Delta\omega} d\omega J(\omega), \quad (27)$$

which follows from Eq. (14) whenever the frequency interval $\Delta\omega$ is chosen around ω_n so that neither of the neighbouring frequencies $\omega_{n\pm 1}$ are contained in it. In order to make sure that the discrete model represents its continuous counterpart faithfully, it is sufficient to require

$$\omega_R^2 = \frac{2}{\pi} \int_0^\infty d\omega \frac{J(\omega)}{\omega} \simeq \sum_{n=1}^N \frac{g_n^2}{\omega_n}. \quad (28)$$

We discuss this point in detail in Appendix E for the Ohmic spectral density with Lorentz-Drude cutoff introduced in Sec. II B, and show that a choice of parameters such that $N \gg \omega_{\max} \gg \omega_c$ guarantees a good agreement.

In Fig. 6(a) we illustrate this calculation for $N = 2000$, $\omega_0 = 0.2$, $\gamma = 0.1$, $\omega_c = 2$, and $\omega_{\max} = 100$, for which $\sum_n g_n^2 / \omega_n \simeq 0.195853 \simeq \omega_R^2 = 0.2$. The nodes of the TIHC corresponding to these parameters can be found to have frequency $\Omega \simeq 57.7278$, while the couplings decay as a power law $G_n \propto n^{-c}$ with almost constant c . Until around $n = 500$, $c \simeq 2$. For $500 \lesssim n \lesssim 1000$, c becomes slightly smaller (i.e., $c \approx 1.77$), although it remains approximately constant. Finally, for $n \gtrsim 1000$, the decay of interactions becomes slower and non-power-law-like. Considering different values of N , we find the above change of behaviour to occur around $N/2$. We are thus dealing with a finite-size effect which does not appear in the thermodynamic limit. In other words, in the thermodynamic limit, the TIHC corresponding to the Ohmic open-system model studied in Ref. [13] becomes a gapless chain with interactions decaying as the square of the distance.

We know from Eq. (19a) that the QFI scales as $\mathcal{F}_T \sim T^2$ at low temperatures in this model. However, we also know that local thermometry on a gapless TIHC should give rise to the

diverging low- T behaviour $\mathcal{F} \sim 1/T^2$, as shown in Sec. III. Therefore, the physical probe must have been delocalized during the mapping onto the TIHC; that way, *local* temperature measurements in the CLM would look *global* on the chain. Below, we will see that this is indeed the case.

Let the Caldeira-Leggett Hamiltonian in Eq. (13) be written as $H_{CL} = \frac{1}{2}(\vec{P}^{CL})^\top \vec{P}^{CL} + \frac{1}{2}(\vec{Q}^{CL})^\top V_{CL} \vec{Q}^{CL}$, and its $N+1$ normal-mode coordinates, as $\vec{q}^{CL} = O_{CL} \vec{Q}^{CL}$. On the other hand, let \vec{q}^C contain the $2N+1$ TIHC normal-mode quadratures $\vec{q}^C = O_C \vec{Q}^C$. We assume that these are ordered in such a way that the first $N+1$ elements of \vec{q}^C correspond to the non-degenerate frequencies $\{\Omega_0, \Omega_1, \dots, \Omega_N\}$. One can thus connect the original CL coordinates with those of the TIHC via $\vec{Q}^{CL} = (O_{CL}^\top \oplus \mathbb{1}_N) O_C \vec{Q}^C$. In particular, the matrix elements $[(O_{CL}^\top \oplus \mathbb{1}_N) O_C]_{1a}$ are the coefficients in the expansion of the position of the probe in terms of the positions of the oscillators in the chain, i.e. $q_0 = \sum_a d_a Q_a$.

We plot this in Fig. 6(b) for the same parameters of Fig. 6(a). We can see that q_0 spreads all over the chain and hence, local manipulations of the probe on the CLM map into complex global measurements on the corresponding TIHC. Notice however, that the resulting low-temperature scaling of the QFI (i.e., $\mathcal{F}_T \sim T^2$) is far worse than what could be achieved by interrogating locally a single node of the chain [cf. Eq. (19b)]. We thus see how local thermometry on a simple linear system can turn into a surprisingly rich problem.

V. CONCLUSIONS

In this paper we have focused on local thermometry on quantum many-body systems, deep into the low temperature regime. First, we proved that the accuracy of local thermometry is exponentially suppressed for any *gapped*, translationally invariant, non-critical and short-range-interacting lattice system. This result is very general and applies to locally-finite as well as harmonic many-body systems.

Furthermore, in order to explore the *gapless* regime, we adopted an open-system approach, and established that thermometry on a harmonic probe coupled to an Ohmic sample is characterized by a distinctive power-law-like low-temperature scaling. Namely, trapped Brownian particles can sense the temperature of a much larger equilibrium sample with a precision scaling as $\sim T^2$. On the contrary, a free probe displays a remarkable diverging scaling of $\sim 1/T^2$. Most importantly, we showed that the decisive factor when switching between exponential and sub-exponentially inefficient quantum thermometry is whether or not the energy spectrum of the global many-body system exhibits a finite gap.

In order to gain further insights into the problem, we studied a simple 1D chain of identical harmonic oscillators with arbitrary interactions and periodic boundary conditions. Our main finding was that the open-system formulation of local thermometry on a single node of a gapped instance of such chain gives rise to a non-standard dissipative model in which the probe is effectively decoupled from the lower-frequency modes of the sample. For the probe to be able to interact with

all the sample modes in the open system description, the 1D chain must be initially gapless. It is intuitively clear that, at sufficiently cold temperatures, those neglected low-frequency modes become dominant. In turn, this explains the exponential suppression of thermal sensitivity in gapped systems.

Remarkably, we demonstrated that local thermometry on a node of a translationally invariant gapless harmonic chain, with *completely arbitrary interactions* (not necessarily short-ranged) is analogous to the problem of estimating the temperature of an *Ohmic sample* with a harmonic probe.

Additionally, we discussed how to discretize and map a continuous open system model of the Caldeira-Leggett type into a translationally invariant harmonic chain. We were thus able to show that the resulting chain exhibits interactions that decay quadratically with the inter-node distance. Finally, we illustrated how, in spite of the necessary existence of a formal open-system-to-chain mapping, the individual Brownian probe needs not correspond to a single node in the chain. Instead, local manipulations of the probe generally look like complex global manipulations on the corresponding chain.

Our results thus shed light from various different angles on the technologically relevant problem of sensing ultra-cold temperatures. Even though we make fundamental statements about the ultimate low-temperature limitations on the precision of temperature measurements, our results have also clear practical implications. Note for instance that the scaling $\sim 1/T^2$ of the sensitivity of a free Brownian particle implies that the relative error $\delta T/T$ can be kept *constant* for arbitrarily low temperatures, by simply tuning the trapping frequency of the thermometer to be sufficiently low. This observation is intimately connected with a recent proposal on low- T thermometry exploiting dynamical control [23].

Our setting is also well suited for tackling other interesting situations, such as local thermometry on gapped *long-range-interacting* systems. In fact, the chain-to-open-system mapping could potentially be exploited to solve such problem *exactly* once the corresponding effective spectral density has been worked out. This issue is worthy of further investigation and will be considered elsewhere.

NOTE ADDED

During the completion of this manuscript, we became aware of the closely related work by P. Hofer *et al.* [35]. In it, the authors argue that gapless spectra allow for sub-exponential low- T scaling of \mathcal{F}_T and work out several examples, including local thermometry in a 1D fermionic chain, which also leads to the scaling $\mathcal{F}_T \sim T^2$.

ACKNOWLEDGMENTS

We gratefully acknowledge funding by the Villum Fonden, European Research Council (ERC) Starting Grant GQCOP (Grant No. 637352), and the COST Action MP1209: ‘‘Thermodynamics in the quantum regime’’.

Appendix A: Heat capacity of local Hamiltonians

In this appendix, we argue that the large-size and low-temperature scaling of the heat capacity of gapped translationally-invariant lattices with finite-range two-body interactions is

$$C(N, T) \leq \mathcal{O}(Ne^{-\Delta/T}). \quad (\text{A1})$$

For harmonic and free-fermion lattices in arbitrary spatial dimensions we prove this in full generality. Although the extensivity is trivial to show also for general lattices with locally finite Hilbert space dimension, the exponential temperature dependence is far more challenging to prove. However, by force of example, we expect Eq. (A1) to hold also in this case.

1. Extensivity

In short-range interacting, translationally-invariant lattice systems with finite local Hilbert space dimension, extensivity of the heat capacity, i.e., that $\lim_{N \rightarrow \infty} C_N/N$ exists and is finite, is a trivial consequence of the fact [37, 38] that, for the partition function of a translationally-invariant system, the limit $\lim_{N \rightarrow \infty} N^{-1} \ln Z_N$ exists and is regular. Indeed, this means that, for $N \gg 1$, $\ln Z_N = \mathcal{O}(N)$, and the extensivity of C_N follows from the identity $C = \beta^2 \partial_\beta^2 \ln Z$.

More intuitively, and, most importantly, also applicable to harmonic lattices, the extensivity can be understood as follows. By representing the lattice by a graph (V_N, E_N) , where V_N is the set of all sites serving as vertices, and E_N , the edges, are the interacting pairs, we write the Hamiltonian as

$$H_N = \sum_{v \in V_N} H_v + \sum_{e \in E_N} h_e, \quad (\text{A2})$$

where H_v are the on-site Hamiltonians, and h_e are the interactions. Since we consider only regular lattices and interactions of finite range, there is only a finite set of edges connected to each vertex. We denote it by E_v and rewrite the Hamiltonian as

$$H_N = \sum_{v \in V_N} \left(H_v + \sum_{e \in E_v} h_e/2 \right) \equiv \sum_{v \in V_N} \tilde{H}_{E_v}, \quad (\text{A3})$$

where \tilde{H}_{E_v} now live in the joint Hilbert space of the vertices at the ends of the edges in E_v . Now, due to the translation-invariance, all operators describing \tilde{H}_{E_v} and corresponding marginal states $\rho_{E_v}^{(N)}$ (note the dependence of the local state on the global system size), albeit residing in different Hilbert spaces, are the same for all v 's. Hence, for the energy of the lattice, we have

$$E_N = N \text{tr}(H_{E_1} \rho_{E_1}^{(N)}). \quad (\text{A4})$$

Finally, by the very definition of the problem, the global state converges when $N \rightarrow \infty$ (see also [37, 38]), and therefore we may formally write $\rho_{E_1}^{(N)} = \rho_{E_1}^{(\infty)} + o(1)$. And since $\rho_{E_1}^{(\infty)}$ is either a finite-component bosonic Gaussian state or a

finite-dimensional positive operator of trace 1, $\text{tr}(H_{E_1} \rho_{E_1}^{(N)}) = e(T) + o(1)$, where $e(T)$, away from criticality, is a regular function of T and is $\mathcal{O}(1)$. Hence, we conclude that $E_N = Ne(T) + o(N)$, which thus proves the extensivity of $C_N = dE_N/dT$. This allows us to define the specific heat $c(T) = \lim_{N \rightarrow \infty} C_N/N$, which we study in the next subsection.

2. Specific heat at low temperatures

Let us first prove Eq. (A1) for harmonic and free-fermion systems. These systems are widely used to describe a wide variety of physical objects, from quantum fields to superconductors (see, e.g., [39]), and are described by Hamiltonians that are bilinear in, respectively, bosonic and fermionic creation and annihilation operators (or can be transformed to such picture, as is the case for the quantum Ising model). Due to bilinearity, such Hamiltonians can always be canonically transformed into ‘‘normal modes’’: $\sum_{n=1}^N \varepsilon_n a_n^\dagger a_n$, where a_n^\dagger and a_n are the bosonic or fermionic creation and annihilation operators, ε_n are the normal mode frequencies, for convenience, ordered increasingly ($\varepsilon_1 \leq \varepsilon_2 \leq \dots$), and N is the number of lattice sites. A fermionic mode is a two-level system and a bosonic mode is an oscillator, therefore, in both bosonic and fermionic cases, the spectral gap, Δ , of the whole system will be equal to ε_1 . Furthermore, since the normal modes do not interact with each other, when the global system is in a thermal state, all of the modes are too. Now, the heat capacity of a single mode is

$$C_n = \frac{(\beta \varepsilon_n)^2 e^{-\beta \varepsilon_n}}{(1 \pm e^{-\beta \varepsilon_n})^2}, \quad (\text{A5})$$

where $--$ is for a bosonic mode and $+$ is for fermionic.

The low-temperature regime is defined as $T \ll \Delta$. Thus, $\beta \varepsilon_n \gg 1$ for all n 's. On the other hand, for sufficiently large arguments, the function in Eq. (A5) is a decreasing function. Hence, for sufficiently low temperatures ($\beta \Delta \geq 4$ would be sufficient),

$$C_N \leq N \frac{(\beta \Delta)^2 e^{-\beta \Delta}}{(1 \pm e^{-\beta \Delta})^2}. \quad (\text{A6})$$

This means that

$$c(T) \leq (\beta \Delta)^2 e^{-\beta \Delta} \cdot \mathcal{O}(1), \quad (\text{A7})$$

which proves Eq. (A1). Moreover, it pinpoints to the fact that one can add a $(\beta \Delta)^\gamma$, where γ would be some system-dependent number, multiplier to Eq. (A1) in order to sharpen the asymptotics. For example, in Appendix A3, we carefully calculate the specific heat for the quantum Ising model, and show that, at low-temperatures, its specific heat scales as $(\beta \Delta)^{3/2} e^{-\beta \Delta}$. In fact, an identical analysis shows that this scaling can be shown to hold for any system that can be decomposed into non-interacting parts so that the dispersion relation is quadratic [40]. Moreover, the scaling $(\beta \Delta)^{3/2} e^{-\beta \Delta}$ was demonstrated for the 1D spin-1/2 XYZ model [41], which is not a free-fermion model. In general, it is common

folklore in solid-state physics that the specific heat in gapped systems decays as $(\beta\Delta)^\gamma e^{-b(\beta\Delta)}$ ($b > 0$) [40, 42–46] (see also similar discussion in Ref. [47]).

3. Low-temperature specific heat of gapped quantum Ising model

Let us illustrate the above result on the simple example of quantum Ising model in a transverse field [48]. It is given by the Hamiltonian

$$H_I = \frac{J}{2} \sum_i \sigma_x^i \otimes \sigma_x^{i+1} - \frac{h}{2} \sum_i \sigma_z^i, \quad (\text{A8})$$

which, in the free-fermion representation [49], takes the form $H_I = \sum_{k=1}^N \varepsilon_k (c_k^\dagger c_k - 1/2)$, where c_k^\dagger and c_k are the creation and annihilation operators of the k -th fermionic mode, and $\varepsilon_k = 2\sqrt{J^2 + h^2 - 2hJ \cos(2\pi k/N)}$, for $k \in \{-\lfloor \frac{N}{2} \rfloor, \dots, \lfloor \frac{N}{2} \rfloor - 1\}$. The smallest gap among the two-level systems and hence the spectral gap of the total system is thus $\Delta = 2|h - J|$. Hence,

$$\varepsilon_k = \Delta \sqrt{1 + \frac{16hJ}{\Delta^2} \sin^2\left(\frac{\pi k}{N}\right)}. \quad (\text{A9})$$

Now, in this representation, the spin chain is a collection of non-interacting two-level systems with different energy gaps. Therefore, the total heat capacity is but the sum of the heat capacities of these two-level systems: $C_N = \sum_k C(\varepsilon_k, T)$, where

$$C(\varepsilon_k, T) = \frac{(\beta\varepsilon_k)^2 e^{-\beta\varepsilon_k}}{(1 + e^{-\beta\varepsilon_k})^2}. \quad (\text{A10})$$

Let us now define

$$k_m = \left\lfloor \frac{N}{\sqrt[3]{\beta\Delta}} \right\rfloor \ll N \quad (\text{A11})$$

and write the heat capacity as

$$C_N = \sum_{k=-k_m}^{k_m} C(\varepsilon_k, T) + \sum_{|k| > k_m} C(\varepsilon_k, T). \quad (\text{A12})$$

Noticing that the second sum is upper-bounded by $(N - 2k_m)C(\varepsilon_{k_m}, T)$, and keeping in mind that we are interested in the regime where $\beta\Delta \gg 1$, we get

$$C_N = \sum_{k=-k_m}^{k_m} C(\varepsilon_k, T) + \mathcal{O}\left(Ne^{-\beta\varepsilon_{k_m}}\right). \quad (\text{A13})$$

Furthermore, since $k_m/N \ll 1$, for $k \leq k_m$, we have

$$\varepsilon_k = \Delta + \frac{8\pi^2 hJ}{\Delta} \frac{k^2}{N^2} + \mathcal{O}\left(\frac{k^4}{N^4}\right) \quad (\text{A14})$$

Further noticing that $(\beta\Delta)k_m^4/N^4 = (\beta\Delta)^{-1/3} \ll 1$ and denoting $f = \frac{8\pi^2 hJ}{\Delta N^2}$, we obtain

$$C_N = (\beta\Delta)^2 e^{-\beta\Delta} \sum_{k=-k_m}^{k_m} \left[1 + \frac{2f}{\Delta} k^2 + \mathcal{O}\left(\frac{k^4}{N^4}\right) \right] e^{-\beta f k^2} + (\text{A15})$$

$$\mathcal{O}\left(Ne^{-\beta\varepsilon_{k_m}}\right). \quad (\text{A16})$$

Finally, noticing that $\beta f k_m^2 = \mathcal{O}\left(\sqrt[3]{\beta\Delta}\right) \gg 1$, the Euler-Maclaurin formula [50] can be written as $\sum_{k=-k_m}^{k_m} e^{-\beta f k^2} = \int_{-k_m}^{k_m} dx e^{-\beta f x^2} + \mathcal{O}\left(e^{-\sqrt[3]{\beta\Delta}}\right)$. Splitting the integral as $\int_{-k_m}^{k_m} = \int_{-\infty}^{\infty} - \int_{k_m}^{\infty} - \int_{-\infty}^{-k_m}$ and noticing that the latter are $\mathcal{O}\left(e^{-\sqrt[3]{\beta\Delta}}\right)$, we obtain that

$$\sum_{k=-k_m}^{k_m} e^{-\beta f k^2} = \pi(\beta f)^{-1/2} + \mathcal{O}\left(e^{-\sqrt[3]{\beta\Delta}}\right). \quad (\text{A17})$$

Deriving the both sides of Eq. (A17) with respect to (βf) once and twice to find, respectively, $\sum_{k=-k_m}^{k_m} k^2 e^{-\beta f k^2}$ and $\sum_{k=-k_m}^{k_m} k^4 e^{-\beta f k^2}$, and substituting them into Eq. (A15), we get

$$C_N = N(\beta\Delta)^{3/2} e^{-\beta\Delta} \sqrt{\frac{\Delta^2}{8hJ}} \left[1 + \mathcal{O}\left(\frac{1}{\beta\Delta}\right) \right], \quad (\text{A18})$$

which, we emphasize, is correct only for $N \gg 1$ and $\beta\Delta \gg 1$.

Appendix B: Getting Eq. (3) from Eq. (2)

Eq. (3) amounts to

$$\begin{aligned} \mathbb{F}(\rho_T, \rho_{T+\delta}) &= 1 - \frac{1}{4} \mathcal{F}_T \delta^2 + \mathcal{O}(\delta^3) \\ &= 1 + \frac{1}{2} \left(\lim_{\delta \rightarrow 0} \frac{\partial^2 \mathbb{F}(\rho_T, \rho_{T+\delta})}{\partial \delta^2} \right) \delta^2 + \mathcal{O}(\delta^3). \end{aligned} \quad (\text{B1})$$

Which holds provided that $\mathbb{F}(\rho_T, \rho_{T+\delta}) = \mathcal{O}(\delta^2)$. To see that this is the case, let us introduce the operator $x := \frac{\partial \rho_T}{\partial T} \delta + \mathcal{O}(\delta^2)$, so that $\rho_{T+\delta} = \rho_T + x$. The Uhlmann fidelity would thus rewrite as $\mathbb{F}(\rho_T, \rho_{T+\delta}) = \left(\text{tr} \sqrt{\sqrt{\rho_T} (\rho_T + x) \sqrt{\rho_T}} \right)^2 = \left(\text{tr} \sqrt{\rho_T^2 + \sqrt{\rho_T} x \sqrt{\rho_T}} \right)^2 := [\text{tr}(\rho_T + y)]^2 = (1 + \text{tr} y)$.

Squaring the definition of this newly-introduced operator y , we see that

$$y^2 + \rho_T y + y \rho_T = \sqrt{\rho_T} x \sqrt{\rho_T}. \quad (\text{B2})$$

Since $x = \mathcal{O}(\delta)$, it is also clear that $y = \mathcal{O}(\delta)$. We can now multiply from left and right by $(\sqrt{\rho_T})^{-1}$, which yields

$$(\sqrt{\rho_T})^{-1} y \sqrt{\rho_T} + \sqrt{\rho_T} y (\sqrt{\rho_T})^{-1} = \frac{\partial \rho_T}{\partial T} \delta + \mathcal{O}(\delta^2). \quad (\text{B3})$$

Note that the *invertibility* is not an issue here, even if ρ_T is not full rank, since all $\mathcal{O}(\delta)$ terms in Eq. (B3) appear multiplied by $\sqrt{\rho_T}$. Taking now the trace of Eq. (B3) one immediately sees that $\text{tr} y = \mathcal{O}(\delta^2)$ and hence, $\mathbb{F}(\rho_T, \rho_{T+\delta}) = 1 + \mathcal{O}(\delta^2)$, as we wanted to verify.

Appendix C: Low-temperature scaling of QFI for arbitrary Ohmic CL models

In this appendix, we intend to find the low-temperature scaling of the QFI of the probe with respect to the sample's temperature T , for Ohmic spectral densities $J(\omega)$ with arbitrary cut-off functions (see Eq. (15) for definition).

Having closed-form formulas for the covariance matrices (Eqs. (16), (16b), and (17)) at hand, let us use the formula [34]

$$\mathbb{F}(\sigma_T, \sigma_{T+\delta}) = \frac{2}{\sqrt{\Lambda + \Delta} - \sqrt{\Lambda}}, \quad (\text{C1})$$

where

$$\Lambda = (4 \det \sigma_T - 1)(4 \det \sigma_{T+\delta} - 1) \quad \text{and} \quad (\text{C2})$$

$$\Delta = 4 \det(\sigma_T + \sigma_{T+\delta}), \quad (\text{C3})$$

to calculate the Uhlmann fidelity between ρ_T and $\rho_{T+\delta}$ directly through their covariance matrices.

Now, writing down the Taylor expansions

$$[\sigma_{T+\delta}]_{11} = [\sigma_T]_{11} + a_1 \delta T + b_1 \delta^2 + \mathcal{O}(\delta^3), \quad (\text{C4})$$

$$[\sigma_{T+\delta}]_{22} = [\sigma_T]_{22} + a_2 \delta + b_2 \delta^2 + \mathcal{O}(\delta^3) \quad (\text{C5})$$

and substituting them into Eqs. (C1), (C2), and (C3), up to the second order in δ , we obtain

$$\mathbb{F}(\sigma_T, \sigma_{T+\delta}) = 1 - \frac{a_1 a_2 + 2[\sigma_T]_{11}^2 a_2^2 + 2[\sigma_T]_{22}^2 a_1^2}{16[\sigma_T]_{11}^2 [\sigma_T]_{22}^2 - 1} \delta^2 + \mathcal{O}(\delta^3).$$

Plugging this into Eq. (3), we obtain that

$$\mathcal{F}(T) = 4 \frac{a_1 a_2 + 2[\sigma_T]_{11}^2 a_2^2 + 2[\sigma_T]_{22}^2 a_1^2}{16[\sigma_T]_{11}^2 [\sigma_T]_{22}^2 - 1}. \quad (\text{C6})$$

This is a very convenient expression in that it does not involve the second-order coefficients in the Taylor expansion of $\sigma_{T+\delta}$ in Eqs. (C4) and (C5). The problem of finding the low-temperature expansion of \mathcal{F} is thus reduced to calculating the low-temperature expansions of $[\sigma_T]_{ii}$ (and a_i will follow as $a_i(T) = d[\sigma_T]_{ii}/dT$).

In the next two subsections, we will extract the low-temperature asymptotics of $\mathcal{F}(T)$ in two (proof-strategy-wise) different cases of $\omega_0 \neq 0$ and $\omega_0 = 0$.

1. The case of a non-free bare probe ($\omega_0 \neq 0$)

Let us start with $[\sigma_T]_{11}$, which is given by (16). Using the identity

$$\coth \frac{x}{2} = 1 + \frac{2}{e^x - 1}, \quad (\text{C7})$$

the expression for $[\sigma_T]_{11}$ can be rewritten as

$$[\sigma_T]_{11} = \sigma_1 + \frac{2}{\pi} \int_0^\infty d\omega \frac{J(\omega)}{|\alpha(\omega)|^2} \frac{1}{e^{\beta\omega} - 1}, \quad (\text{C8})$$

where

$$\sigma_1 = \frac{1}{\pi} \int_0^\infty d\omega \frac{J(\omega)}{|\alpha(\omega)|^2}. \quad (\text{C9})$$

Let us now switch to dimensionless parameters via the transformations

$$\omega \rightarrow \frac{\omega}{\omega_C} \quad \text{and} \quad T \rightarrow \frac{T}{\omega_C}, \quad (\text{C10})$$

where ω_C is the cut-off frequency. For a general form of the spectral density, ω_C can be fixed to be the frequency maximizing $J(\omega)$ as a function of ω (cf., e.g., Fig. ??). After the transformation, Eq. (C8) turns into

$$\sigma_{11} = \sigma_1 + \frac{2\omega_C}{\pi} \int_0^\infty d\omega \frac{J(\omega\omega_C)}{|\alpha(\omega\omega_C)|^2} \frac{1}{e^{\beta\omega} - 1}, \quad (\text{C11})$$

where now T and ω are dimensionless and we have dropped the subscript T in σ to simplify the notation. By making the substitution $\beta\omega = A$ in the integration variable in Eq. (C11), we arrive at

$$\sigma_{11} = \sigma_1 + \frac{2T\omega_C}{\pi} \int_0^\infty dA \frac{J(AT\omega_C)}{|\alpha(AT\omega_C)|^2} \frac{1}{e^A - 1}. \quad (\text{C12})$$

Since we are interested in $T \ll 1$ expansion of σ_{11} , let us now turn to $\alpha(\omega)$'s behaviour near $\omega = 0$. Keeping in mind the definition of Cauchy principal value, Eq. (C10), and that $\omega > 0$, let us rewrite the expression for $\chi(\omega)$ (see Eq. (17)) as

$$\pi\chi(\omega\omega_C) = \int_0^\infty d\omega' \frac{J(\omega_C\omega')}{\omega' + \omega} + \quad (\text{C13})$$

$$\lim_{\varepsilon \rightarrow 0} \left[\int_0^{\omega-\varepsilon} d\omega' \frac{J(\omega'\omega_C)}{\omega' - \omega} + \int_{\omega+\varepsilon}^\infty d\omega' \frac{J(\omega'\omega_C)}{\omega' - \omega} \right]. \quad (\text{C14})$$

Or, equivalently,

$$\pi\chi(\omega\omega_C) = \int_\omega^\infty \frac{dx}{x} J(\omega_C(x - \omega)) + \quad (\text{C15})$$

$$\lim_{\varepsilon \rightarrow 0} \left[\int_\varepsilon^\infty \frac{dx}{x} J(\omega_C(\omega + x)) - \int_\varepsilon^\omega \frac{dx}{x} J(\omega_C(\omega - x)) \right]. \quad (\text{C16})$$

Let us now split the first integral in Eq. (C16) into $\int_\varepsilon^\omega + \int_\omega^\infty$ and notice that, since $\omega \ll 1$, whenever $\varepsilon < \omega$ and $x \in [\varepsilon, \omega]$, we can write $J(\omega_C(\omega + x)) = J(\omega_C\omega) + J'(\omega_C\omega)\omega_C x + \mathcal{O}(\omega_C^2 x^2)$. This allows us to rewrite Eqs. (C15), (C16) as

$$\pi\chi(\omega\omega_C) = \int_\omega^\infty \frac{dx}{x} [J(\omega_C(x - \omega)) + J(\omega_C(\omega + x))] + \quad (\text{C17})$$

$$2J'(\omega)\omega_C\omega + \omega_C^2 \mathcal{O}(\omega^2), \quad (\text{C18})$$

where, in the last line, we used $J'(\omega_C\omega) = J'(\omega) + \omega_C\omega\mathcal{O}(1)$.

Let us now take a closer look at the integral in Eq. (C17) by Taylor-expanding the nominator of its integrand around $\omega_C x$:

$$\begin{aligned} \int_\omega^\infty \frac{dx}{x} [J(\omega_C(x - \omega)) + J(\omega_C(\omega + x))] = \\ 2 \int_\omega^\infty \frac{dx}{x} J(\omega_C x) + \omega_C^2 \omega^2 \int_\omega^\infty \frac{dx}{x} J''(\omega_C x) + \omega_C^4 J^{(4)}(0) \mathcal{O}(\omega^4), \end{aligned} \quad (\text{C19})$$

where, in the last term, we kept $J^{(4)}(0)$, which has dimensionality of $[\text{time}]^2$, in order to explicitly account for the fact that the whole expression has dimensionality of $[\text{time}]^{-2}$. In those cases when the order of magnitude of this quantity can be relevant, for example, when ω_C is described by a large number (although one has to be careful here as ω_C is a dimensional quantity), we shall invoke Eq. (15) and calculate $\omega_C^4 J^{(4)}(\Omega) = \omega_C \gamma \left[4f^{(3)}\left(\frac{\Omega}{\omega_C}\right) + \frac{\Omega}{\omega_C} f^{(4)}\left(\frac{\Omega}{\omega_C}\right) \right]$. Now, given the rapid decay of $f(x)$ for $x > 1$, it is obvious that the expression in the brackets is $\mathcal{O}(1)$ (e.g., for the standard choice of $f(x) = e^{-x}$, the object in the brackets is bounded by -4 from below and e^{-5} from above). Hence, $\omega_C^4 J^{(4)}(0) \mathcal{O}(\omega^4)$ can be considered to be $\omega_C^2 \mathcal{O}(\omega^4)$. We will take this into account during our further steps. Coming back to Eq. (C19), let us observe that

$$\int_{\omega}^{\infty} \frac{dx}{x} J(\omega_C x) = \int_0^{\infty} \frac{dx}{x} J(\omega_C x) - \int_0^{\omega} \frac{dx}{x} J(\omega_C x) = \frac{\pi}{2} \omega_R^2 - J'(0) \omega_C \omega + \omega_C^2 \mathcal{O}(\omega^2) \quad (\text{C20})$$

and

$$\int_{\omega}^{\infty} \frac{dx}{x} J''(\omega_C x) = \int_{\omega}^{1/K} \frac{dx}{x} J''(\omega_C x) + \int_{1/K}^{\infty} \frac{dx}{x} J''(\omega_C x) = \int_{\omega}^{1/K} \frac{dx}{x} J''(\omega_C x) + \mathcal{O}(1), \quad (\text{C21})$$

where we need to choose K such that, within the segment $[0, \omega_C/K]$, $J(\omega)$ is linear within a good approximation. In particular, it will be sufficient for our purposes to choose K so that, for x in $[\omega, 1/K]$, $\frac{1}{2} J''(0) \leq J''(\omega_C x) \leq \frac{3}{2} J''(0)$. Such a finite, Hamiltonian-dependent K has to exist by the very assumption of $J(\omega)$ being Ohmic. Having so chosen K , we thus obtain

$$\int_{\omega}^{1/K} \frac{dx}{x} J''(\omega_C x) = -\mathcal{O}(1) J''(0) \ln \omega + \mathcal{O}(1). \quad (\text{C22})$$

As regards the fact of the second integral in Eq. (C21) being $\mathcal{O}(1)$, it can be straightforwardly seen by noticing that $\frac{J''(\omega_C x)}{x} = \frac{\gamma}{\omega_C} \left[2 \frac{f'(x)}{x} + f''(x) \right]$ and recalling that $f(x)$ is a well-behaved function of x that rapidly decays for $x > 1$.

Collecting what we have obtained so far, we find that

$$\chi(\omega \omega_C) = \omega_R^2 + \mathcal{O}(1) \omega_C^2 \omega^2 \ln \omega, \quad (\text{C23})$$

and, substituting this into Eq. (17), we finally arrive at

$$\alpha(\omega \omega_C) = \omega_0^2 - \mathcal{O}(1) \omega_C^2 \omega^2 \ln \omega - i \omega_C^2 \omega \mathcal{O}(1), \quad (\text{C24})$$

which leaves us with

$$|\alpha(\omega \omega_C)|^2 = \omega_0^4 + \mathcal{O}(1) \omega_C^4 \omega^2 \left[1 + \frac{\omega_0^2}{\omega_C^2} \ln \omega \right]. \quad (\text{C25})$$

One needs to keep in mind that this holds only in the limit of $\omega \ll 1$.

Now, from Eq. (C25) it follows that $\lim_{\omega \rightarrow 0} |\alpha(\omega \omega_C)|^2 = \omega_0^4 > 0$, which guarantees the convergence of σ_1 (see

Eq. (C9)). We further obtain from Eq. (C25) that

$$\frac{J(TA\omega_C)}{|\alpha(TA\omega_C)|^2} = \frac{T\omega_C J'(0)A[1 + \mathcal{O}(AT)]}{\omega_0^4 + \mathcal{O}(1)\omega_C^4 A^2 T^2 \left[1 + \frac{\omega_0^2}{\omega_C^2} \ln(AT) \right]}, \quad (\text{C26})$$

and, substituting this into Eq. (C12), we get

$$\sigma_{11} = \sigma_1 + \quad (\text{C27})$$

$$T^2 \frac{2J'(0)}{\pi \omega_C^2} \int_0^{\infty} \frac{dA}{e^A - 1} \cdot \frac{A[1 + \mathcal{O}(AT)]}{\frac{\omega_0^4}{\omega_C^4} + \mathcal{O}(1)A^2 T^2 \left[1 + \frac{\omega_0^2}{\omega_C^2} \ln(AT) \right]}. \quad (\text{C28})$$

Noticing that the multiplier of $\mathcal{O}(1)$ in the denominator can be absorbed into the $1 + \mathcal{O}(AT)$ standing in the nominator, we arrive at

$$\sigma_{11} = \sigma_1 + T^2 \frac{2J'(0)}{\pi \omega_C^2} \int_0^{\infty} \frac{dA}{e^A - 1} \frac{A}{\frac{\omega_0^4}{\omega_C^4} + \mathcal{O}(AT)}. \quad (\text{C29})$$

Conducting an identical analysis for σ_{22} yields

$$\sigma_{22} = \sigma_2 + T^4 \frac{2J'(0)}{\pi} \int_0^{\infty} \frac{dA}{e^A - 1} \frac{A^3}{\frac{\omega_0^4}{\omega_C^4} + \mathcal{O}(AT)}, \quad (\text{C30})$$

where

$$\sigma_2 = \frac{1}{\pi} \int_0^{\infty} d\omega \frac{\omega^2 J(\omega)}{|\alpha(\omega)|^2}. \quad (\text{C31})$$

Looking at the denominator of the integrands in Eqs. (C29) and (C30), we see that the low-temperature limit has three distinct regimes: $T \ll \frac{\omega_0^4}{\omega_C^4}$, $\frac{\omega_0^4}{\omega_C^4} \ll 1$ while $T \sim \frac{\omega_0^4}{\omega_C^4}$, and $1 \gg T \gg \frac{\omega_0^4}{\omega_C^4}$. We study these regimes separately.

a. The regime of $T \ll \frac{\omega_0^4}{\omega_C^4}$

This regime is the most relevant one, especially in lattice systems. Indeed, in those cases, the highest normal frequency, ω_{\max} , of the reservoir is of the same order as the local frequency of the lattice sites (see Sec. IV), and, since $\omega_C < \omega_{\max}$, we conclude that $\frac{\omega_0}{\omega_C} = \mathcal{O}(1)$, which automatically implies $T \ll \frac{\omega_0^4}{\omega_C^4}$ as $T \ll 1$. Moreover, the condition $T \ll 1$ is equivalent to the physical temperature, $T\omega_C$, being $\ll \omega_0$. In those cases when $\omega_0 \ll \omega_C$, this condition becomes more subtle. However it is important to note that $J(\omega)$ characterizes the strength with which the probe interacts with a reservoir's mode of frequency ω (see Eq. (14)). Therefore, even if the sample has large-frequency normal modes, a strong coupling between the probe and the high-frequency modes of the sample would be an exotic situation. This means that ω_C cannot be too large. So, for not very small ω_0 's, the condition $T \ll \frac{\omega_0^4}{\omega_C^4}$ would again be equivalent to the physical temperature, $\omega_C T$, being $\ll \omega_0$.

In light of the above, and the fact that $\int_0^\infty dA \frac{A}{e^A - 1} = \frac{\pi^2}{6}$ and $\int_0^\infty dA \frac{A^3}{e^A - 1} = \frac{\pi^4}{15}$, we have

$$\sigma_{11} = \sigma_1 + \frac{\pi}{3} \frac{\omega_c^2 J'(0)}{\omega_0^4} T^2 [1 + \mathcal{O}(T)] \quad (\text{C32})$$

and

$$\sigma_{22} = \sigma_2 + \frac{2\pi^3}{15} \frac{\omega_c^4 J'(0)}{\omega_0^4} T^4 [1 + \mathcal{O}(T)]. \quad (\text{C33})$$

Lastly, calculating the derivatives of σ_{11} and σ_{22} with respect to T so as to obtain a_1 and a_2 , we substitute everything into Eq. (C6) and end up with

$$\mathcal{F}(\omega_c T) = \frac{32\pi^2}{144\sigma_1^2\sigma_2^2 - 9} \frac{\sigma_2^2 J'(0)^2}{\omega_0^8} \omega_c^2 T^2 [1 + \mathcal{O}(T)], \quad (\text{C34})$$

which, coming back to the physical temperature, means that

$$\mathcal{F}(T) \propto T^2. \quad (\text{C35})$$

b. The regime when $\frac{\omega_0^4}{\omega_c^4} \ll 1$ while $T \sim \frac{\omega_0^4}{\omega_c^4}$

To determine the behaviour of σ_{11} and σ_{22} in this case, let us recall that the integrands are of the form as given by Eqs. (C29) and (C30) only for $AT \ll 1$. On the other hand, whenever $e^A \gg [\frac{\omega_0^4}{\omega_c^4} + \mathcal{O}(AT)]$, the actual form of $J/|\alpha|^2$ does not play a significant role. Luckily, these two regimes are easily combined. Indeed, when $\frac{\omega_c^4}{\omega_0^4} \gg A \gg \ln \frac{\omega_c^4}{\omega_0^4}$, we have both $AT \ll 1$ and $e^A \gg [\frac{\omega_0^4}{\omega_c^4} + \mathcal{O}(AT)]$ satisfied (keep in mind that $T \sim \omega_0^4/\omega_c^4$). Let us denote $\kappa = \frac{\omega_0^4}{\omega_c^4} \ll 1$, and choose some L such that $\frac{1}{\kappa} \gg L \gg \ln \frac{1}{\kappa}$, for example, $L = \kappa^{-\frac{1}{2}}$. We can now split

$$\int_0^\infty \frac{dA}{e^A - 1} \cdot \frac{A}{\frac{\omega_0^4}{\omega_c^4} + \mathcal{O}(AT)} = \left[\int_0^L + \int_L^\infty \right] \frac{dA}{e^A - 1} \cdot \frac{A}{\kappa + \mathcal{O}(AT)}. \quad (\text{C36})$$

The second term is dominated by the exponent, and can be trivially shown to be $\mathcal{O}(\kappa^{-1}e^{-L})$ and is hence exponentially small. We will neglect it from now on. As per the first term, keeping in mind that $\frac{T}{\kappa} = \mathcal{O}(1)$, we can rewrite it as

$$\frac{1}{\kappa} \int_0^L \frac{dA}{e^A - 1} \frac{A}{1 + A\mathcal{O}(1)}. \quad (\text{C37})$$

Since $L \gg 1$, up to exponentially small terms, the integral can be extended to ∞ , and, upon observing that the integrand is regular at $A = 0$, we obtain that

$$\int_0^\infty \frac{dA}{e^A - 1} \frac{A}{\frac{\omega_0^4}{\omega_c^4} + \mathcal{O}(AT)} = \frac{\mathcal{O}(1)}{\kappa}, \quad (\text{C38})$$

which means that

$$\sigma_{11} = \sigma_1 + T \frac{J'(0)}{\omega_c^2} \mathcal{O}(1). \quad (\text{C39})$$

In order to be able to estimate the derivative of σ_{11} precisely, instead of differentiating the integrand in Eq. (C29), one can differentiate the integrand in Eq. (C28). By doing so, one obtains that the T -derivative of the integral in Eq. (C28) is $\frac{\mathcal{O}(1)}{\kappa}$. Hence, we have that

$$a_1 = \frac{J'(0)}{\omega_c^3} \mathcal{O}(1). \quad (\text{C40})$$

By the same logic, we obtain that

$$\sigma_{22} = \sigma_2 + T^3 J'(0) \mathcal{O}(1) \quad (\text{C41})$$

and

$$a_2 = T^2 \frac{J'(0)}{\omega_c} \mathcal{O}(1). \quad (\text{C42})$$

Plugging these formulas into Eq. (C6), we get

$$\mathcal{F}(\omega_c T) = \frac{\mathcal{O}(1)}{16\sigma_1^2\sigma_2^2 - 9} \frac{\sigma_2^2 J'(0)^2}{\omega_c^6}. \quad (\text{C43})$$

It is furthermore straightforward to check that neither σ_1 nor σ_2 have special dependence on κ . Therefore, we conclude that

$$\mathcal{F}(\omega_c T) = \frac{\sigma_2^2 J'(0)^2}{\omega_c^6} \mathcal{O}(1). \quad (\text{C44})$$

c. The regime of $1 \gg T \gg \frac{\omega_0^4}{\omega_c^4}$

To find how σ_{11} scales in this case, let us split the integral in Eq. (C29) as follows:

$$\int_0^\infty \frac{dA}{e^A - 1} \cdot \frac{A}{\frac{\omega_0^4}{\omega_c^4} + \mathcal{O}(AT)} = \left[\int_0^{\frac{\kappa}{T}} + \int_{\frac{\kappa}{T}}^\infty \right] \frac{dA}{e^A - 1} \cdot \frac{A}{\kappa + \mathcal{O}(AT)}. \quad (\text{C45})$$

Keeping in mind that $\frac{\kappa}{T} \ll 1$, for the first integral, we can write:

$$\int_0^{\frac{\kappa}{T}} \frac{dA}{A(1 + \mathcal{O}(A))} \cdot \frac{A}{\kappa + \kappa\mathcal{O}(1)} = \frac{\mathcal{O}(1)}{\kappa} \int_0^{\frac{\kappa}{T}} dA = \frac{\mathcal{O}(1)}{T}. \quad (\text{C46})$$

For the second integral, we have

$$\int_{\frac{\kappa}{T}}^\infty \frac{dA}{e^A - 1} \cdot \frac{A}{AT\mathcal{O}(1)} = \frac{\mathcal{O}(1)}{T} \int_{\frac{\kappa}{T}}^\infty \frac{dA}{e^A - 1} = \frac{\mathcal{O}(1)}{T} \ln \frac{T}{\kappa}. \quad (\text{C47})$$

Combining these, we obtain

$$\sigma_{11} = \sigma_1 + \frac{J'(0)}{\omega_c^2} \mathcal{O}(1) T \ln \frac{T}{\kappa}. \quad (\text{C48})$$

As in the previous subsection, in order to not miss any important dependencies on T , to find a_1 , we first calculate the T -derivative of the integral in Eq. (C28). Taking the derivative of the integrand and splitting the integral as above, we obtain that the derivative is $\frac{\mathcal{O}(1)}{T}$. Therefore, calculating the T -derivative of the whole expression in Eq. (C28), we end up with

$$a_1 = \frac{J'(0)}{\omega_C^3} \mathcal{O}(1) \ln \frac{T}{\kappa}. \quad (\text{C49})$$

Note that, as in the previous subsection, we would obtain the same result were we to formally differentiate Eq. (C48) with respect to T .

Via a similar calculation, we obtain

$$\sigma_{22} = \sigma_2 + T^3 J'(0) \mathcal{O}(1) \quad (\text{C50})$$

and

$$a_2 = T^2 \frac{J'(0)}{\omega_C} \mathcal{O}(1). \quad (\text{C51})$$

Eq. (C6) then yields

$$\mathcal{F}(\omega_C T) = \frac{\sigma_2^2 J'(0)^2}{\omega_C^6} \left(\ln \frac{T}{\omega_0^4 / \omega_C^4} \right)^2 \mathcal{O}(1). \quad (\text{C52})$$

2. The case of a free bare probe ($\omega_0 = 0$)

The analysis in the previous subsection does not entirely apply in this case due to the fact that, whenever $\omega_0 = 0$, $\alpha(0) = 0$ and $\alpha(\omega)$ scales around 0 in such a way that the integrals defining σ_1 and σ_2 diverge.

In order to find the quantum Fisher information, we need to regularize these divergences. We do so by recalling that, in our analysis, we first take the limit $N \rightarrow \infty$, where N is the number of the constituents of the sample, and only then consider the physics of $T \rightarrow 0$. Now, no sample is strictly infinite, and this implies that there exists a minimal frequency in the system (an "infrared cut-off"). Indeed, in the illustrative case of the sample being a d -dimensional cube, the spatial dimensions are given by $L \propto N^{1/d}$. And to this length scale, a minimal energy and hence a minimal frequency, Ω , scaling as $L^{-2} = N^{-2/d}$, can be associated. Therefore, instead of 0, the integrals in Eqs. (16) and (16b) have to start from Ω , which, abstracting from the example of the cube above, is now a formal parameter controlling the size of the sample and is to be taken to 0 before any other limit. Note that Ω does not need to have the specific scaling with N mentioned above.

The above implies that, in order to determine $\mathcal{F}(T)$, one has to fix T to some value and calculate $\lim_{\Omega \rightarrow 0} \mathcal{F}(T, \Omega)$.

From the expression for α in Eq. (C24), we immediately see that, for $\omega \ll 1$,

$$|\alpha(\omega \omega_C)|^2 = \omega_C^4 \omega^2 \mathcal{O}(1). \quad (\text{C53})$$

Let us furthermore write the $\mathcal{O}(1)$ above as $W^{-1} + o(1)$, with W being some T -independent constant composed of $J'(0)$ and

ω_C . In what follows, we will absorb all other constants, such as $J'(0)$ and ω_C , into W .

We now pick a constant $0 < \varepsilon \ll 1$ and make the following splitting:

$$\sigma_{11} = \frac{\omega_C}{\pi} \left[\int_{\Omega}^{\varepsilon} + \int_{\varepsilon}^{\infty} \right] d\omega \frac{J(\omega \omega_C)}{|\alpha(\omega \omega_C)|^2} \frac{e^{\beta \omega} + 1}{e^{\beta \omega} - 1}. \quad (\text{C54})$$

The second integral is non-singular and hence is $\mathcal{O}(1)$ with respect to the limit $\Omega \rightarrow 0$. Whereas for the first integral, simple algebra brings us to

$$TW \int_{\Omega}^{\varepsilon} d\omega \frac{1 + o(1)}{\omega^2} = \frac{WT}{\Omega} [1 + o(1)], \quad (\text{C55})$$

where, again, $o(1)$ is with respect to the limit $\Omega \rightarrow 0$. We thus have that

$$\sigma_{11} = \frac{WT}{\Omega} [1 + o(1)] \quad (\text{C56})$$

and, after taking the derivative and regrouping the $\mathcal{O}(1)$ terms,

$$a_1 = \frac{W}{\Omega} [1 + o(1)]. \quad (\text{C57})$$

Analogously, we obtain

$$\sigma_{22} = W'T [1 + o(1)] \quad (\text{C58})$$

and

$$a_2 = W'[1 + o(1)]. \quad (\text{C59})$$

The expression for the quantum Fisher information, (C6), thus leads to

$$\mathcal{F}(T \omega_C, \Omega) = T^{-2} \omega_C^{-2} [1 + o(1)], \quad (\text{C60})$$

which, after taking the $\Omega \rightarrow 0$ limit and going back from the rescaled temperature (see Eq. (C10)) to the physical temperature, leaves us with

$$\mathcal{F}(T) = T^{-2} \quad (\text{C61})$$

for any temperature. For the error bar of the temperature measurements, δT , we thus have

$$\frac{\delta T}{T} \leq \frac{1}{\sqrt{M}}, \quad (\text{C62})$$

where M is the number of independent trials. In other words, if one makes measurements on a single node of a gapless TIHC, the error bar δT will scale as T .

Appendix D: Spectrum of 1D harmonic chain

Let us show that, whenever G_n decays as n^{-s} (with some $s > 0$) or faster, the gap between the ground state and the first excited state of the chain Hamiltonian of Eq. (??) is

$$\Delta_N^2 = \Omega^2 - 2 \sum_{n=1}^{\infty} (-1)^{n-1} G_n + \mathcal{O}(\max\{N^{-s}, N^{-2}\}). \quad (\text{D1})$$

This quantity coincides with the lowest normal frequency of the Hamiltonian and, as can immediately be seen from Eq. (21), for monotonically decreasing G_n 's, the smallest Ω_a is Ω_N . This brings us to

$$\Delta_N^2 = \Omega^2 - 2 \sum_{n=1}^{\infty} (-1)^{n-1} G_n + \delta_N, \quad (\text{D2})$$

where

$$\delta_N = 4 \sum_{n=1}^N (-1)^{n-1} G_n \left(\sin \frac{\pi n}{4N+2} \right)^2 + \sum_{n=N+1}^{\infty} (-1)^n G_n. \quad (\text{D3})$$

Regrouping this as $\sum_n (-1)^{n-1} X_n = \sum_n (X_n - X_{n+1})$ and keeping in mind that $\sin^2 x - \sin^2 y = \sin(x-y) \sin(x+y)$, we arrive at

$$\delta_N = 4 \sum_n (G_n - G_{n+1}) \left(\sin \frac{\pi n}{4N+2} \right)^2 - \quad (\text{D4})$$

$$4 \sum_n G_{n+1} \sin \frac{\pi}{4N+2} \sin \frac{\pi(2n+1)}{4N+2} + \sum_{n=N+1}^{\infty} (-1)^n G_n. \quad (\text{D5})$$

Now, using the inequality $\sin x \leq x$, for the first series, we have

$$4 \sum_n (G_n - G_{n+1}) \left(\sin \frac{\pi n}{4N+2} \right)^2 \leq \sum_n \frac{(G_n - G_{n+1}) n^2 \pi^2}{(2N+1)^2},$$

and, keeping in mind that, since G_n decays as n^{-s} or faster, $(G_n - G_{n+1}) \leq \mathcal{O}(n^{-s-1})$, we conclude that

$$\sum_n (G_n - G_{n+1}) \left(\sin \frac{\pi n}{4N+2} \right)^2 = \frac{1}{N^2} \sum_{n=1}^{N/2} \mathcal{O}(N^{1-s}) \quad (\text{D6})$$

$$= \mathcal{O}(\max\{N^{-s}, N^{-2}\}). \quad (\text{D7})$$

We do the same in the second series, and, taking $G_n \leq \mathcal{O}(n^{-s})$ into account, we obtain that it is also $\mathcal{O}(\max\{N^{-s}, N^{-2}\})$. Finally, we notice that $0 \leq |\sum_{n=N+1}^{\infty} (-1)^n G_n| = |G_{N+1} - \sum_{n=N+2}^{\infty} (G_n - G_{n+1})| \leq G_{N+1}$, which shows that the last series in Eq. (D3) is $\leq \mathcal{O}(N^{-s})$. This concludes the proof of Eq. (D1).

Let us also mention that the maximal normal frequency corresponds to $a = 0$ in Eq. (21), and is given by

$$\Omega_{\max}^2 = \Omega^2 + 2 \sum_{n=1}^N G_n. \quad (\text{D8})$$

It thus scales as N^{1-s} when $0 < s < 1$ and as $\ln N$ when $s = 1$, whereas for G_n decaying faster than n^{-1} , Ω_{\max} is of the same order of magnitude as Ω .

Lastly, we note, in passing, that, since, when $s \geq 1$, for $\omega \ll 1$, $J(\omega) \sim \omega$, $g_n^2 \sim \omega_n^2$, which, in turn, means that

$$g_n \propto n^{-1/2}. \quad (\text{D9})$$

Appendix E: Consistency of the discretization of a continuous CL model

In order for the renormalization frequency ω_R^2 defined by the discrete formula

$$\omega_R^2 = \sum_n g_n^2 / \omega_n^2 = \sum_n \int_{\Delta\omega_n} d\omega \frac{J(\omega)}{\pi\omega_n} \quad (\text{E1})$$

to be equal to the one given by the continuous formula

$$\omega_R^2 = \int_0^{\infty} d\omega \frac{J(\omega)}{\pi\omega}, \quad (\text{E2})$$

at least all the intervals $\Delta\omega_n$ have to be contiguous and thereby fill the whole interval of $(0, +\infty)$. To proceed, let us upper-bound the the probe can couple to by some $\omega_{\max} > \omega_C$. Moreover, let us assume that the ω 's are distributed equidistantly:

$$\omega_n = \frac{\omega_{\max}}{N} n. \quad (\text{E3})$$

Then,

$$g_n^2 = \frac{\omega_{\max}}{\pi N} n \int_{\frac{\omega_{\max}}{N}(n-\frac{1}{2})}^{\frac{\omega_{\max}}{N}(n+\frac{1}{2})} d\omega J(\omega). \quad (\text{E4})$$

For our example of Ohmic spectral density with Lorentz-Drude cut-off, $J(\omega) = 2\gamma\omega\omega_C^2/(\omega^2 + \omega_C^2)$, we have

$$\begin{aligned} g_n^2 &= \frac{\omega_{\max}}{\pi N} n \gamma \omega_C^2 \ln \frac{\left(\frac{\omega_{\max}}{\omega_C N}\right)^2 \left(n + \frac{1}{2}\right)^2 + 1}{\left(\frac{\omega_{\max}}{\omega_C N}\right)^2 \left(n - \frac{1}{2}\right)^2 + 1} \\ &= \frac{2\gamma^2 \left(\frac{\omega_{\max}}{N}\right)^3}{\left(\frac{\omega_{\max}}{\omega_C N} n\right)^2 + 1} + \mathcal{O}\left(\frac{\omega_{\max}^4 n^2}{\omega_C^4 N^4}\right) \approx \frac{\omega_n}{\pi} J_1(\omega_n) \Delta\omega. \end{aligned} \quad (\text{E5}) \quad (\text{E6})$$

Interestingly, since the intervals shrink as N^{-1} , the dependency of g_n on $\Delta\omega$ is there to mimic precisely the feature of general TIHCs given by (D9).

Now, it is easy to that

$$\omega_R^2 = \sum_{n=1}^N \rightarrow \int_0^{\infty} d\omega \frac{J(\omega)}{\pi\omega} = \gamma\omega_C \quad (\text{E7})$$

provided that

$$N \gg \omega_{\max} \gg \omega_C. \quad (\text{E8})$$

Indeed,

$$\sum_{n=1}^N \frac{g_n^2}{\omega_n^2} = \frac{2\gamma}{\pi} \frac{\omega_{\max}}{N} \sum_{n=1}^N \left(\frac{\omega_{\max}^2}{\omega_C^2 N^2} n^2 + 1 \right)^{-1} + \mathcal{O}\left(\frac{\omega_{\max}^2}{\omega_C^4 N}\right), \quad (\text{E9})$$

and, using the identity [50]

$$\sum_{n=1}^{\infty} (a^2 n^2 + 1)^{-1} = \frac{\pi}{2a} \coth \frac{\pi}{a} - \frac{1}{2} \quad (\text{E10})$$

and noticing via Euler-Maclaurin formula [50] that

$$\sum_{n=N+1}^{\infty} \left(\frac{\omega_{\max}^2}{\omega_C^2 N^2} n^2 + 1 \right)^{-1} = \frac{\omega_C N}{\omega_{\max}} \left(\frac{\pi}{2} - \arctan \frac{\omega_{\max}}{\omega_C} \right) + \mathcal{O}(1),$$

we finally arrive at

$$\omega_R^2 = \gamma\omega_C + \mathcal{O}\left(\frac{\omega_C^2}{\omega_{\max}}\right) + \mathcal{O}\left(\frac{\omega_{\max}^2}{N}\right), \quad (\text{E11})$$

which holds for $N \gg \omega_{\max} \gg \omega_C$. Note that if any of these relations is broken, ω_R^2 can significantly differ from $\int_0^{\infty} d\omega \frac{J(\omega)}{\pi\omega}$.

- [1] L. Carlos and F. Palacio, *Thermometry at the Nanoscale: Techniques and Selected Applications*, Vol. 38 (Royal Society of Chemistry, 2015).
- [2] P. Neumann, I. Jakobi, F. Dolde, C. Burk, R. Reuter, G. Waldherr, J. Honert, T. Wolf, A. Brunner, J. H. Shim, *et al.*, *High-precision nanoscale temperature sensing using single defects in diamond*, *Nano letters* **13**, 2738 (2013).
- [3] G. Kucsko, P. Maurer, N. Yao, M. Kubo, H. Noh, P. Lo, H. Park, and M. Lukin, *Nanometre-scale thermometry in a living cell*, *Nature* **500**, 54 (2013).
- [4] L. A. Correa, M. Mehboudi, G. Adesso, and A. Sanpera, *Individual Quantum Probes for Optimal Thermometry*, *Phys. Rev. Lett.* **114**, 220405 (2015).
- [5] M. Mehboudi, M. Moreno-Cardoner, G. D. Chiara, and A. Sanpera, *Thermometry precision in strongly correlated ultracold lattice gases*, *New J. Phys.* **17**, 055020 (2015).
- [6] A. De Pasquale, D. Rossini, R. Fazio, and V. Giovannetti, *Local quantum thermal susceptibility*, *Nat. Comm.* **7**, 12782 (2016).
- [7] M. G. A. Paris, *Achieving the Landau bound to precision of quantum thermometry in systems with vanishing gap*, *J. Phys. A: Math. Theor.* **49**, 03LT02 (2016).
- [8] D. Halbertal, J. Cuppens, M. B. Shalom, L. Embon, N. Shadmi, Y. Anahory, H. Naren, J. Sarkar, A. Uri, Y. Ronen, *et al.*, *Nanoscale thermal imaging of dissipation in quantum systems*, *Nature* **539**, 407 (2016).
- [9] S. M. Kay, *Fundamentals of statistical signal processing* (Prentice Hall PTR, 1993).
- [10] S. L. Braunstein and C. M. Caves, *Statistical distance and the geometry of quantum states*, *Phys. Rev. Lett.* **72**, 3439 (1994).
- [11] D. Reeb and M. M. Wolf, *Tight bound on relative entropy by entropy difference*, *IEEE Trans. Inf. Theory* **61**, 1458 (2015).
- [12] A. Einstein, *Die plancksche theorie der strahlung und die theorie der spezifischen wärme*, *Annalen der Physik* **327**, 180 (1906).
- [13] L. A. Correa, M. Perarnau-Llobet, K. V. Hovhannisyán, S. Hernández-Santana, M. Mehboudi, and A. Sanpera, *Enhancement of low-temperature thermometry by strong coupling*, *Phys. Rev. A* **96**, 062103 (2017).
- [14] G. De Palma, A. De Pasquale, and V. Giovannetti, *Universal locality of quantum thermal susceptibility*, *Phys. Rev. A* **95**, 052115 (2017).
- [15] K. Eckert, A. Sanpera, M. Lewenstein, E. Polzik, *et al.*, *Quantum polarization spectroscopy of ultracold spinor gases*, *Phys. Rev. Lett.* **98**, 100404 (2007).
- [16] K. Eckert, O. Romero-Isart, M. Rodriguez, M. Lewenstein, E. S. Polzik, and A. Sanpera, *Quantum non-demolition detection of strongly correlated systems*, *Nature Phys.* **4**, 50 (2008).
- [17] M. Mehboudi, L. A. Correa, and A. Sanpera, *Achieving sub-shot-noise sensing at finite temperatures*, *Phys. Rev. A* **94**, 042121 (2016).
- [18] Y. Subaşı, C. H. Fleming, J. M. Taylor, and B. L. Hu, *Equilibrium states of open quantum systems in the strong coupling regime*, *Phys. Rev. E* **86**, 061132 (2012).
- [19] U. Weiss, *Quantum dissipative systems*, 2nd ed. (World Scientific, 1999).
- [20] A. O. Caldeira and A. J. Leggett, *Path integral approach to quantum Brownian motion*, *Physica A* **121**, 587 (1983).
- [21] P. Riseborough, P. Hanggi, and U. Weiss, *Exact results for a damped quantum-mechanical harmonic oscillator*, *Phys. Rev. A* **31**, 471 (1985).
- [22] H. Grabert, U. Weiss, and P. Talkner, *Quantum theory of the damped harmonic oscillator*, *Z. Phys. B* **55**, 87 (1984).
- [23] V. Mukherjee, A. Zwick, A. Ghosh, and G. Kurizki, *High precision multi-temperature quantum thermometry via dynamical control*, arXiv preprint arXiv:1711.09660 (2017).
- [24] A. Uhlmann, *The “transition probability” in the state space of a-algebra*, *Reports on Mathematical Physics* **9**, 273 (1976).
- [25] A. García-Saez, A. Ferraro, and A. Acín, *Local temperature in quantum thermal states*, *Phys. Rev. A* **79**, 052340 (2009).
- [26] M. Kliesch, C. Gogolin, M. J. Kastoryano, A. Riera, and J. Eisert, *Locality of Temperature*, *Phys. Rev. X* **4**, 031019 (2014).
- [27] S. Hernández-Santana, A. Riera, K. V. Hovhannisyán, M. Perarnau-Llobet, L. Tagliacozzo, and A. Acín, *Locality of temperature in spin chains*, *New J. Phys.* **17**, 085007 (2015).
- [28] M. A. Nielsen and I. L. Chuang, *Quantum computation and quantum information* (Cambridge University Press, Cambridge, England, 2010).
- [29] A. Ferraro, A. García-Saez, and A. Acín, *Intensive temperature and quantum correlations for refined quantum measurements*, *Europhys. Lett.* **98**, 10009 (2012).
- [30] M. Cramer and J. Eisert, *Correlations, spectral gap and entanglement in harmonic quantum systems on generic lattices*, *New J. Phys.* **8**, 71 (2006).
- [31] L. A. Correa, A. A. Valido, and D. Alonso, *Asymptotic discord and entanglement of nonresonant harmonic oscillators under weak and strong dissipation*, *Phys. Rev. A* **86**, 012110 (2012).
- [32] A. A. Valido, A. Ruiz, and D. Alonso, *Quantum correlations and energy currents across three dissipative oscillators*, *Phys. Rev. E* **91**, 062123 (2015).
- [33] H. Bateman, *Tables of integral transforms (vol. II)*, California Institute of Technology Bateman Manuscript Project, New York: McGraw-Hill, 1954, edited by Erdelyi, Arthur **1** (1954).
- [34] H. Scutaru, *Fidelity for displaced squeezed thermal states and the oscillator semigroup*, *J. Phys. A: Math. Gen.* **31**, 3659 (1998).
- [35] P. Hofer, J. B. Brask, and N. Brunner, *Fundamental limits on low-temperature quantum thermometry*, arXiv:quant-ph/1711.09827.
- [36] R. M. Gray, *Toeplitz and Circulant Matrices: A Review*, *Found. Trends Commun. Inf. Theory* **2**, 155 (2006).
- [37] H. Araki, *Gibbs states of a one dimensional quantum lattice*, *Commun. Math. Phys.* **14**, 120 (1969).
- [38] H. Araki, *On the equivalence of the KMS condition and the variational principle for quantum lattice systems*, *Commun. Math. Phys.* **38**, 1 (1974).
- [39] X.-G. Wen, *Quantum field theory of many-body systems* (Oxford University Press, New York, 2004).
- [40] F. Heiniger, E. Bucher, and M. J., *Low temperature specific heat of transition metals and alloys*, *Phys. kondens. Materie* **5**, 243 (1966).
- [41] M. Takahashi, *Low-temperature specific heat of spin-1/2 anisotropic Heisenberg ring*, *Prog. Theor. Phys.* **50**, 1519 (1973).
- [42] W. S. Corak, B. B. Goodman, C. B. Satterthwaite, and A. Wexler, *Exponential temperature dependence of the electronic specific heat of superconducting vanadium*, *Phys. Rev.* **96**, 1442 (1954).
- [43] H. M. Rosenberg, *Low Temperature Solid State Physics* (Oxford University Press, Oxford, 1963).
- [44] T. Chakraborty and P. Pietiläinen, *Specific heat of quantum Hall systems*, *Phys. Rev. B* **55**, R1954 (1997).
- [45] N. H. van Dijk, F. Bourdarot, J. C. P. Klaasse, I. H. Hagmusa,

- E. Brück, and A. A. Menovsky, *Specific heat of heavy-fermion Uru_2Si_2 in high magnetic fields*, *Phys. Rev. B* **56**, 14493 (1997).
- [46] Y. Wang, B. Revaz, A. Erb, and A. Junod, *Direct observation and anisotropy of the contribution of gap nodes in the low-temperature specific heat of $Yb_2Cu_3O_7$* , *Phys. Rev. B* **63**, 094508 (2001).
- [47] F. G. S. L. Brandão and M. Cramer, *Entanglement area law from specific heat capacity*, *Phys. Rev. B* **92**, 115134 (2015).
- [48] E. Lieb, T. Schultz, and D. Mattis, *Two soluble models of an antiferromagnetic chain*, *Ann. Phys.* **16**, 407 (1961).
- [49] S. Sachdev, *Quantum phase transitions* (Cambridge University Press, Cambridge, England, 2011).
- [50] G. M. Fikhtengol'ts, *A course in differential and integral calculus*, Vol. 2 (Nauka, Moscow, 1969).